Title

A State-of-the-Science Review of Arsenic's Effects on Glucose Homeostasis in Experimental Models

Journal

Environmental Health Perspectives, 128(1)

ISSN

1542-4359

Authors

Castriota, Felicia
Rieswijk, Linda
Dahlberg, Sarah
et al.

Publication Date

2020

DOI

10.1289/ehp4517

Peer reviewed

A Section 508–conformant HTML version of this article is available at https://doi.org/10.1289/EHP4517.

A State-of-the-Science Review of Arsenic's Effects on Glucose Homeostasis in Experimental Models

Felicia Castriota,[1] Linda Rieswijk,[1] Sarah Dahlberg,[1] Michele A. La Merrill,[2] Craig Steinmaus,[1] Martyn T. Smith,[1] and Jen-Chywan Wang[1,3]

[1]Superfund Research Program, University of California, Berkeley, California, USA
[2]Department of Environmental Toxicology, University of California, Davis, California, USA
[3]Department of Nutritional Sciences & Toxicology, University of California, Berkeley, California, USA

Background: The prevalence of type 2 diabetes (T2D) has more than doubled since 1980. Poor nutrition, sedentary lifestyle, and obesity are among the primary risk factors. While an estimated 70% of cases are attributed to excess adiposity, there is an increased interest in understanding the contribution of environmental agents to diabetes causation and severity. Arsenic is one of these environmental chemicals, with multiple epidemiology studies supporting its association with T2D. Despite extensive research, the molecular mechanism by which arsenic exerts its diabetogenic effects remains unclear.

Objectives: We conducted a literature search focused on arsenite exposure *in vivo* and *in vitro*, using relevant end points to elucidate potential mechanisms of oral arsenic exposure and diabetes development.

Methods: We explored experimental results for potential mechanisms and elucidated the distinct effects that occur at high vs. low exposure. We also performed network analyses relying on publicly available data, which supported our key findings.

Results: While several mechanisms may be involved, our findings support that arsenite has effects on whole-body glucose homeostasis, insulin-stimulated glucose uptake, glucose-stimulated insulin secretion, hepatic glucose metabolism, and both adipose and pancreatic β-cell dysfunction.

Discussion: This review applies state-of-the-science approaches to identify the current knowledge gaps in our understanding of arsenite on diabetes development. https://doi.org/10.1289/EHP4517

Introduction

Arsenic is a naturally occurring metalloid in the earth's crust, found in water, air, food, and soil (Hughes et al. 2011). More than 200 million individuals are exposed to arsenic in drinking water, with high prevalence in Taiwan, Bangladesh, India, South America, and the United States (Hughes et al. 2011). The principal route of arsenic exposure occurs via the ingestion of contaminated drinking water and food, which continues to be a widespread public health concern (ATSDR 2007). Foods that have been reported to have high levels of inorganic arsenic include rice and rice-based products, poultry, apple juice, wine, and beer (Castriota et al. 2018). Runoff and leaching from rocks, sediment, and anthropogenic sources are significant processes of drinking water contamination (ATSDR 2007). Oral inorganic arsenic exposure has been reported in epidemiological studies to be associated with a wide range of diseases, including cancers of the skin, bladder, lung, kidney, and liver, in addition to developmental, dermatological, neurological, respiratory, immune, cardiovascular, endocrine, and metabolic disorders (Hughes et al. 2011; Naujokas et al. 2013). Additional studies have been published to further investigate the association between arsenic and type 2 diabetes (T2D) (Castriota et al. 2018; Farzan et al. 2017; Grau-Perez et al. 2017; Pan et al. 2013; Peng et al. 2015).

Elemental arsenic is present in both inorganic and organic forms and in various oxidative states (Hughes et al. 2011). Both the pentavalent form, arsenate (iAs^{V}) and the trivalent form, arsenite (iAs^{III}) have been detected in drinking water (Hughes et al. 2011). After oral exposure, arsenite metabolism in humans occurs primarily in the liver via arsenic (+3 oxidation state) methyltransferase (As3MT) and involves sequential reduction and methylation reactions that lead to the formation of both trivalent and pentavalent monomethylated (MMA) and dimethylated (DMA) metabolites (Agusa et al. 2011). A reductive methylation model has been proposed where trivalent metabolites are conjugated to glutathione (GSH) and ultimately oxidized to pentavalent arsenical metabolites (MMA^{V+} and DMA^{V+}) as the final products (Hayakawa et al. 2005; Agusa et al. 2011). In recent years, the production of trivalent methylated species has been evaluated and deemed a bioactivation process that increases an individual's susceptibility to arsenic toxicity (Agusa et al. 2011; ATSDR 2007). Methylarsonous (MMA^{III+}) and dimethylarsinous acids (DMA^{III+}) have been found to be cytotoxic (Hou et al. 2013) and genotoxic (Petrick et al. 2000; Styblo et al. 2000) in both murine and human cell lines.

Studies have attempted to distinguish the risk of arsenic-induced T2D based on exposure level with inconsistent results across experimental models. In 2012, an expert panel assembled by the National Toxicology Program (NTP) deemed evidence for animal research on the topic of arsenic and diabetes inconclusive due to the dissimilarity of animal exposures across studies and to those reported in human exposure studies (Maull et al. 2012). The concentration of arsenite in drinking water used in published *in vivo* metabolic studies have ranged from 100 ppb up to 50 ppm (Ditzel et al. 2016; Garciafigueroa et al. 2013; Adebayo et al. 2015; Druwe et al. 2012; Paul et al. 2011; Song et al. 2017; Maull et al. 2012). *In vivo* studies have large discrepancies in exposure duration, concentration, and administration, many of which do not mimic those observed in human populations worldwide (Huang et al. 2011; Maull et al. 2012; Navas-Acien et al. 2005; Thayer et al. 2012). Treatment with arsenite *in vitro* is also highly variable with regard to both dose and duration (Maull et al. 2012). In light of these concerns, the expert panel recommended that future arsenic

Address correspondence to Jen-Chywan Wang, 315 Morgan, Department of Nutritional Sciences & Toxicology, University of California, Berkeley, Berkeley, CA 94720-3104, USA. Telephone: (510) 643-1039. Email: Walwang@berkeley.edu

Supplemental Material is available online (https://doi.org/10.1289/EHP4517).
The authors declare they have no actual or potential competing financial interests.
Received 27 September 2018; Revised 22 November 2019; Accepted 26 November 2019; Published 3 January 2020.

research focus on animal studies designed to mimic internal doses observed in humans, accompanied by low-dose *in vitro* studies on cell lines involved in glucose metabolism (Maull et al. 2012; Thayer et al. 2012).

This review highlights key *in vivo* studies with supporting associations observed *in vitro*. This targeted approach relies on quantitative methodologies to qualitatively synthesize the most relevant studies and address inconsistencies in arsenical species, route of administration, and duration of exposure that are reported in the literature. We provide mechanistic evidence to support epidemiologic findings and advance our understanding of arsenic and T2D development.

Methods

Literature Search

We performed a literature review search using PubMed through the Health Assessment Workspace Collaborative (HAWC) Literature Search tool (https://hawcproject.org/) to locate studies focusing specifically on arsenite exposure and T2D. Using the HAWC database, we searched PubMed for manuscripts through 17 October 2019, using the following search terms: ("Arsenite" OR "Arsenic" AND "Type 2 Diabetes") OR ("Arsenite" OR "Arsenic" AND "Insulin") OR ("Arsenite" OR "Arsenic" AND "Adipogenesis") OR ("Arsenite" OR "Arsenic" AND "Glucose Transport") OR ("Arsenite" OR "Arsenic" AND "Liver") OR ("Arsenite" OR "Arsenic" AND "Skeletal Muscle") OR ("Arsenite" OR "Arsenic" AND "Pancreatic beta cells") OR ("Arsenite" OR "Arsenic" AND "Chronic"). Both arsenic and arsenite were included as search terms to reduce the possibility of missing a potential manuscript that fulfilled our inclusion criteria. HAWC allows researchers to perform a PubMed database literature search where studies from the results of the query are imported and tagged for either inclusion or exclusion.

Study Selection

All studies underwent an identical tagging process and were screened using specified inclusion and exclusion criteria. The inclusion criteria for experimental studies and literature reviews required reporting of both exposure to arsenite and T2D. These criteria were established based on the research question of interest, which focused on the effect of oral arsenite exposure either in mice, rodent or human cell lines relevant to T2D to assess the effect of the chemical on mechanisms involved in dysregulation of glucose homeostasis. The exclusion criteria for experimental studies and literature reviews were that *a*) they were administered a chemical other than the trivalent form of arsenite, *b*) studies were conducted in humans, *c*) studies were "reviews" or "commentaries", *d*) studies with *in utero* exposure only, *e*) studies relied on nonrodent animal models, *f*) included arsenicals as a mixture, or *g*) the assessment of the target organ or cell line was not relevant to glucose homeostasis or T2D development.

Study Characterization

The study tagging was conducted by three researchers (F.C., L.R., and S.D.), and any inconsistencies were resolved by consensus. HAWC was used to manage the study selection process and create a literature Tag-tree that illustrates study identification and classification (Figure 1). We referred to the NTP Office of Health Assessment and Translation (OHAT)'s risk-of-bias rating tool to assess the quality of the animal studies included in this review (OHAT 2015). A total of 15 animal studies were rated for each of the 9 risk-of-bias questions outlined for animal studies by OHAT's guidelines (OHAT 2015). The risk-of-bias rating was based on a four-point scale, which included definitively low risk of bias (++), probably low risk of bias (+), probably high risk of bias not reported (−/NR), and definitely high risk of bias (–). Based on our assessment, there is a low probability of risk of bias (Figures S1 and S2).

Network Analyses

In addition to the literature review, we also relied on chemical- and disease-related gene association data using the publicly available Comparative Toxicogenomics Database (CTD) (MDI Biological Laboratory 2019) to identify genes that are associated with arsenic and T2D (Davis et al. 2017). Within CTD, chemicals and diseases are annotated with medical subject headings (MeSH) identifiers that facilitate searching within the database. Our CTD analysis was conducted using MeSH identifiers for sodium arsenite (MeSH: C017947), insulin resistance (MeSH: D007333), and T2D (MeSH: D003924).

To further investigate the biological processes enriched for the list of genes obtained, we used the ClueGO app (Bindea et al. 2009) within Cytoscape (version summer 2018; Cytospace Consortium) (Lotia et al. 2013) together with the WikiPathways repository (WikiPathways 2018; Slenter et al. 2018). Cytoscape is able to visualize molecular interaction networks and integrate these with gene expression profiles and other data. Additional features are available as applications. For gene set enrichment analysis (GSEA), we used the WikiPathways repository (WikiPathways 2018) containing 418 curated human pathways and 5,866 human genes. Using the ClueGO application within Cytoscape together with GSEA enabled the visualization of nonredundant and highly connected pathways in one functionally grouped network. Pathway selection criteria included a minimum number or percentage of genes (at least three genes or 4% of the total). The selection of highly connected pathways was based on kappa statistics (kappa score >0.4). In this way, functionally related biological pathways (containing the same genes) were clustered together.

Results

We identified 4,831 manuscripts from a PubMed search in HAWC using MeSH terms related to arsenite and T2D. After exclusion of 4,784 manuscripts, 47 were used in the final review (Figure 1; Excel Table S1, highlighted in red). The included manuscripts were comprised of 15 animal studies and 32 mechanistic studies. Based on our review of the current literature, we propose biological mechanisms to explain the association between arsenic exposure and dysregulation of glucose homeostasis. We further explore and validate published *in vivo* and *in vitro* targets via the use of network analyses from publicly available data. After individual gene lists were obtained, we identified 16 genes commonly affected by sodium arsenite, insulin resistance, and T2D (Figure 2).

Whole-Body Glucose Homeostasis

Overall, *in vivo* mouse studies show that impaired glucose tolerance has been observed only under exposure to high doses of arsenic, such as 50 ppm (Figure 3). Figure 3 provides a graphical representation of whole-body glucose homeostasis and insulin resistance observed in the *in vivo* studies reviewed on arsenite exposure. Figure 3 reveals that exposure to lower doses of arsenic, such as 4.9 ppm and below, does not seem to alter glucose homeostasis in mice unless combined with genetic-induced diabetic models.

In vivo studies found impaired glucose tolerance in mice treated at high levels (in the range of parts per million) of arsenite. Persistent impaired glucose tolerance was observed in 8-wk-old C57BL/6J male mice based on glucose tolerance tests performed (Kirkley et al. 2017). In two studies by Paul et al.

comparing 25- and 50-ppm 8-wk arsenite treatment found that 4-wk-old C57BL/6J male mice developed impaired glucose tolerance only at the highest exposure dose (Paul et al. 2007, 2008). While a relatively lower dose (3 ppm) of arsenite treatment for 16 wk did not affect glucose tolerance in 7-wk-old nondiabetic C57BLKS/J$^{db/m}$ male mice, such treatment increased susceptibility to impaired glucose tolerance in 7-wk-old diabetic C57BKS/Lepr$^{db/db}$ male mice (Liu et al. 2014).

Studies in genetic obese C57BKS/Lepr$^{db/db}$ male mice suggest the potential for a synergistic interaction between arsenic exposure and nutritional overload on the development of metabolic disorders. We identified four rodent studies that assessed the effects of arsenic coexposures with a high-fat diet (Ditzel et al. 2016; Paul et al. 2011; Wu et al. 2008; Tan et al. 2011). Swiss Webster mice were treated with arsenic (100 ppb) after weaning for 10 wk (to 13 wk of age) (Ditzel et al. 2016). During the course of treatment, a high-fat diet was administered to assess the effects on fatty liver disease. Ectopic fatty lipid deposition and liver damage were observed in these mice (Ditzel et al. 2016). However, despite the induction of hepatic fibrosis, no significant rise in homeostatic model assessment for insulin resistance (HOMA-IR), a measure of insulin resistance, was observed (Figure 3). (Ditzel et al. 2016). However, when mice were

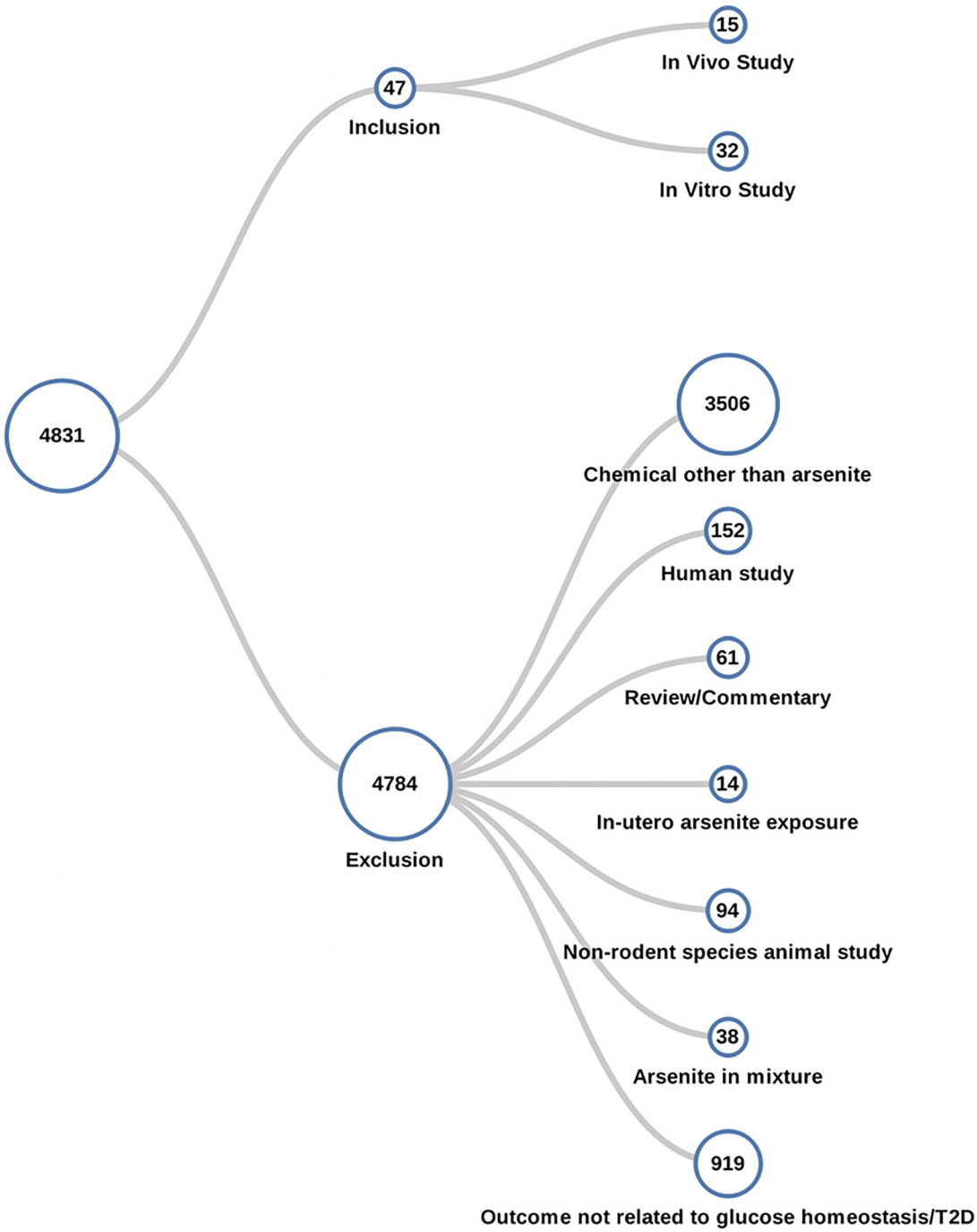

Figure 1. Literature Tag-tree illustrating the number of included and excluded studies based on author study characterization. We used relevant medical subject headings (MeSH) terms and targeted searches using PubMed with literature tagging and visualization tools from the Health Assessment Workspace Collaborative (HAWC) Project (hawcproject.org/).

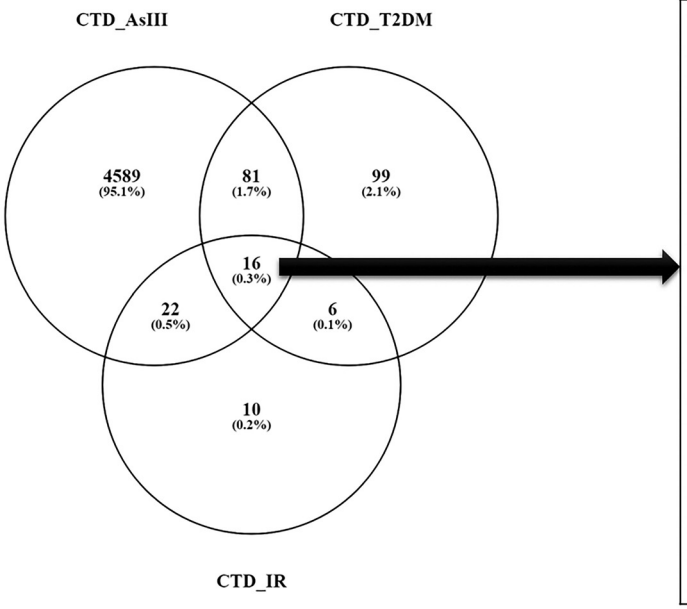

Gene Symbol	Gene description
ADIPOQ	Adiponectin, C1Q and collagen domain containing
C3	Complement C3
EGFR	Epidermal growth factor receptor
HMOX1	Heme oxygenase 1
INS	Insulin
INS1	Insulin I
IRS1	Insulin receptor substrate 1
IRS2	Insulin receptor substrate 2
LEP	Leptin
LEPR	Leptin receptor
NOS3	Nitric oxide synthase 3
PPARG	Peroxisome proliferator activated receptor gamma
SIRT1	Sirtuin 1
SLC2A4	Solute carrier family 2 member 4
SOD2	Superoxide dismutase 2
TNF	Tumor necrosis factor

Figure 2. Chemical- and disease-related gene association data. Findings were obtained by searching the publicly available Comparative Toxicogenomics Database (CTD) (MDI Biological Laboratory 2019) using medical subject headings (MeSH) identifiers for sodium arsenite (iAs^{III+}) (MeSH:C017947), insulin resistance (MeSH: D007333), and type 2 diabetes (T2D) (MESH: D003924). On the left, a Venn diagram is shown depicting the overlapping genes between the different gene sets. On the right, 16 genes are presented. Venn diagrams were created using Venny (version 2.1; BioinfoGP). Note: CTD_As III, sodium arsenite–associated genes obtained from the CTD; CTD_IR, insulin resistance–associated genes obtained from the CTD; CTD_T2DM, type 2 diabetes mellitus–associated genes obtained from the CTD.

exposed to arsenic from embryonic day 5 to 13 wk of age and also fed a high-fat diet after weaning, the effects on hepatic lipid accumulation and fibrosis were even more pronounced, and HOMA-IR was significantly elevated (Ditzel et al. 2016). These findings elucidate important differences for *in utero* vs. postnatal arsenic dosing.

Insulin-Stimulated Glucose Uptake and Glucose Transport

Insulin is an anabolic hormone secreted by pancreatic β cells in response to high blood glucose levels. One of the major functions of insulin is to promote glucose uptake and utilization in peripheral tissues, such as skeletal muscle and white adipose tissue. During insulin resistance, the ability of insulin to promote glucose utilization in skeletal muscle and white adipose tissue is impaired (Saltiel and Kahn 2001).

Using 3T3-L1 adipocytes as a model, 4 h sodium arsenite treatment at 20 μM (2.6 ppm) and 100 μM (13 ppm) decreased insulin-stimulated and basal glucose uptake (Walton et al. 2004). At 50 μM (6.5 ppm) arsenite, 4 h of exposure significantly reduced both insulin-stimulated phosphorylated protein kinase B (AKT) levels and the expression of AKT protein (Walton et al. 2004). Similar concentration-dependent effects on insulin-stimulated glucose uptake (ISGU) were observed with the metabolites methylarsine oxide and iododimethylarsine (Walton et al. 2004). Notably, the authors did not examine whether 20 μM of arsenite treatment for 4 h was sufficient to alter AKT expression. Xue et al. treated 3T3-L1 adipocytes with 0.25–2 μM (32–260 ppb) arsenite for 7 d (Xue et al. 2011). The authors observed decreased insulin-stimulated AKT phosphorylation on serine residue 473, a hallmark of AKT activation. A significant reduction in ISGU was noted at 2 μM arsenite treatment, although a decreasing trend in glucose uptake was observed starting at lower concentrations (0.25–1 μM) (Xue et al. 2011). These responses were correlated to a dose-dependent increase in intracellular GSH and the expression of nuclear factor-erythroid 2-related factor 2 (NRF2), which is a central transcription factor regulating cellular adaptive response to oxidative stress (Xue et al. 2011). NRF2 activity was shown to reduce insulin-stimulated AKT phosphorylation and glucose transporter type 4 (GLUT4) translocation in white adipose tissue of leptin deficient $(Lep)^{ob/ob}$ mice (Xu et al. 2012).

Padmaja Divya et al. treated 3T3-L1 preadipocytes and C2C12 myoblasts with 0.5, 1, and 2 μM arsenite for 8 wk. At the end of treatment, cells were differentiated to either adipocytes or myotubes (Padmaja Divya et al. 2015). All three concentrations decreased ISGU (Padmaja Divya et al. 2015). While 0.5 μM of arsenite showed no significant reduction in the expression of GLUT4 in 3T3-L1 adipocytes or C2C12 myotubes, both 1 and 2 μM arsenite decreased GLUT4 expression in these cell lines (Padmaja Divya et al. 2015). Mitochondrial membrane potential was also altered in 2 μM arsenite treatment in both 3T3-L1 adipocytes and C2C12 myotubes (Padmaja Divya et al. 2015). This observation coincided with the decreased expression of protein deacetylase sirtuin 3 (SIRT3) and the recruitment of forkhead box O3 (FOXO3A), a transcription factor that regulates reactive oxygen species (ROS) metabolism, to its binding sites in the manganese superoxide dismutase (MnSOD) and peroxisome proliferator-activated receptor-gamma coactivator 1 alpha (PGC1α) genes (Sundaresan et al. 2009). Overexpression of SIRT3 and MnSOD in C2C12 myotubes enhanced mitochondrial membrane potential and restored ISGU (Padmaja Divya et al. 2015). Interestingly, SIRT3 appeared to deacetylate FOXO3A, MnSOD, and PGC1α (Padmaja Divya et al. 2015). Arsenic exposure in C2C12 myoblasts led to the deacetylation of FOXO3A at the lysine 100 residue, which promoted FOXO3A's nuclear localization and subsequent inactivation (Padmaja Divya et al. 2015). These *in vitro* findings elucidated arsenite's role in inhibiting SIRT3–FOXO3A signaling and reducing mitochondrial activity, thereby impairing ISGU (Padmaja Divya et al. 2015).

Arsenite exposure has widespread metabolic effects, also influencing peripheral glucose uptake in the central nervous system

A.

Reference	Study Type	Diet	Species of mice	Dose (ppm)	Reported Endpoint	Consolidated Endpoint
Ditzel et al. 2016	In utero (ED5) + 13-week chronic	TestDiet Western Diet (40.1% Fat)	Swiss Webster	0.1	HOMA-IR	Insulin resistance
	13-week chronic	TestDiet Western Diet (40.1% Fat)	Swiss Webster	0.1	HOMA-IR	Insulin resistance
Liu et al. 2014	16-week chronic	Standard chow (20% Protein)	C57BLKS/J db/m	3	HOMA-%B	Insulin resistance
	16-week chronic	Standard chow (20% Protein)	C57BKS/Lepr db/db	3	HOMA-%B	Insulin resistance
	16-week chronic	Standard chow (20% Protein)	C57BKS/Lepr db/db	3	HOMA-IR	Insulin resistance
	16-week chronic	Standard chow (20% Protein)	C57BKS/Lepr db/db	3	ITT	Insulin resistance
	16-week chronic	Standard chow (20% Protein)	C57BKS/Lepr db/db	3	Blood insulin (pmol/L)	Insulin resistance
	16-week chronic	Standard Chow (20% Protein)	C57BKS/Lepr db/db	3	PCK1 (Gluconeogenesis)	Insulin resistance
	16-week chronic	Standard Chow (20% Protein)	C57BKS/Lepr db/db	3	Na+K+-ATPase	Insulin resistance
	16-week chronic	Standard chow (20% Protein)	C57BLKS/J db/m	3	HOMA-IR	Insulin resistance
	16-week chronic	Standard chow (20% Protein)	C57BLKS/J db/m	3	ITT	Insulin resistance
	16-week chronic	Standard chow (20% Protein)	C57BLKS/J db/m	3	Blood insulin (pmol/L)	Insulin resistance
	16-week chronic	Standard Chow (20% Protein)	C57BLKS/J db/m	3	PCK1 (Gluconeogenesis)	Insulin resistance
	16-week chronic	Standard Chow (20% Protein)	C57BLKS/J db/m	3	Na+K+-ATPase	Insulin resistance
Lee et al. 2014	8-week subchronic	Standard chow diet	C57BL/6 db/db	10	ITT	Insulin resistance
Zuo et al. 2019	17-week chronic	Chow diet (Jiangsu Xietong Organism, Co)	C57BL/6J	5	ITT	Insulin resistance
	17-week chronic	Chow diet (Jiangsu Xietong Organism, Co)	C57BL/6J	20	ITT	Insulin resistance
Song et al. 2017	18-week chronic	Standard chow (20% Protein)	C57BL/6J	5	Serum insulin (mU/L)	Insulin resistance
	18-week chronic	Standard chow (20% Protein)	C57BL/6J	50	Serum insulin (mU/L)	Insulin resistance
Kirkley et al. 2017	8-week subchronic	Teklad Global Diet 2018 (18% Protein)	C57BL/6J	50	HOMA-IR	Insulin resistance
	8-week subchronic	Teklad Global Diet 2018 (18% Protein)	C57BL/6J	50	Δ insulin AUC / Δ glucose AUC from 0-10 mins during IP-GTT	Insulin resistance
Rodríguez et al. 2016	1-month subchronic	Labdiet 5001 (23% Protein)	C57BL/6J	50	GLUT1, GLUT3	Insulin resistance
	1-month subchronic	Labdiet 5001 (23% Protein)	C57BL/6J	50	Insulin mRNA	Insulin resistance

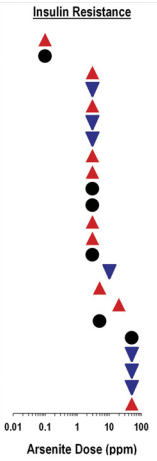

B.

Reference	Study Type	Diet	Species of mice	Dose (ppm)	Reported Endpoint	Consolidated Endpoint
Liu et al. 2014	16-week chronic (db/m)	Standard chow (20% Protein)	C57BLKS/J db/m	3	GTT	Blood glucose (mg/dL)
	16-week chronic (db/db)	Standard chow (20% Protein)	C57BKS/Lepr db/db	3	GTT	Blood glucose (mg/dL)
	16-week chronic (db/db)	Standard chow (20% Protein)	C57BKS/Lepr db/db	3	Blood glucose (mg/dL)	Blood glucose (mg/dL)
	16-week chronic (db/db)	Standard chow (20% Protein)	C57BLKS/J db/m	3	Blood glucose (mg/dL)	Blood glucose (mg/dL)
Lee et al. 2014	8-week subchronic	Standard chow diet	C57BL/6 db/db	10	Blood glucose AUC, fasting blood glucose AUC, HbA1C	Blood glucose (mg/dL)
Zuo et al. 2019	17-week chronic	Chow diet (Jiangsu Xietong Organism, Co)	C57BL/6J	5	GTT	Blood glucose (mg/dL)
	17-week chronic	Chow diet (Jiangsu Xietong Organism, Co)	C57BL/6J	20	GTT	Blood glucose (mg/dL)
Song et al. 2017	18-week chronic	Standard chow (20% Protein)	C57BL/6J	5	Serum glucose (mmol/L)	Blood glucose (mg/dL)
	18-week chronic	Standard chow (20% Protein)	C57BL/6J	50	Serum glucose (mmol/L)	Blood glucose (mg/dL)
Paul et al. 2007	8-week subchronic	Lab Diet 5058 (21.8% Protein)	C57BL/6J	25	GTT	Blood glucose (mg/dL)
	8-week subchronic	Lab Diet 5058 (21.8% Protein)	C57BL/6J	50	GTT	Blood glucose (mg/dL)
Kirkley et al. 2017	8-week subchronic	Teklad Global Diet 2018 (18% Protein)	C57BL/6J	50	GTT	Blood glucose (mg/dL)
	8-week subchronic	Teklad Global Diet 2018 (18% Protein)	C57BL/6J	50	% Blood glucose	Blood glucose (mg/dL)
	8-week subchronic	Teklad Global Diet 2018 (18% Protein)	C57BL/6J	50	Blood glucose (mg/dL)	Blood glucose (mg/dL)

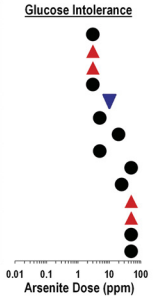

C.

Reference	Study Type	Diet	Species of mice	Dose (ppm)	Reported Endpoint	Consolidated Endpoint
Adebayo et al. 2015	5-week subchronic	AIN76A (21.5% Protein)	C57BL/6J	0.1	WAT weight (mg)	Adipose Tissue Weight
	5-week subchronic	AIN76A (21.5% Protein)	C57BL/6J	0.1	Liver weight (mg)	Liver Weight
Ditzel et al. 2016	In utero (ED5) + 13-week chronic	TestDiet Western Diet (40.1% Fat)	Swiss Webster	0.1	Liver to body ratio	Liver Weight
	13-week chronic	TestDiet Western Diet (40.1% Fat)	Swiss Webster	0.1	Liver to body ratio	Liver Weight
Liu et al. 2014	16-week chronic	Standard chow (20% Protein)	C57BLKS/J db/m	3	Liver (g/100g BW)	Liver Weight
	16-week chronic	Standard chow (20% Protein)	C57BKS/Lepr db/db	3	Liver (g/100g BW)	Liver Weight
	16-week chronic	Standard chow (20% Protein)	C57BLKS/J db/m	3	Pancreas (g/100g BW)	Pancreas Weight
	16-week chronic	Standard chow (20% Protein)	C57BKS/Lepr db/db	3	Pancreas (g/100g BW)	Pancreas Weight
Zuo et al. 2019	17-week chronic	Chow diet (Jiangsu Xietong Organism, Co)	C57BL/6J	5	Brown adipose tissue mass	Adipose Tissue Weight
Song et al. 2017	18-week chronic	Standard chow (20% Protein)	C57BL/6J	5	Fat mass (g)	Adipose Tissue Weight
	18-week chronic	Standard chow (20% Protein)	C57BL/6J	5	Fat mass / Body mass (%)	Adipose Tissue Weight
	18-week chronic	Standard chow (20% Protein)	C57BL/6J	5	Serum adiponectin (ug/mL)	Adipose Tissue Weight
	18-week chronic	Standard chow (20% Protein)	C57BL/6J	50	Fat mass (g)	Adipose Tissue Weight
	18-week chronic	Standard chow (20% Protein)	C57BL/6J	50	Fat mass / Body mass (%)	Adipose Tissue Weight
Kirkley et al. 2017	8-week subchronic	Teklad Global Diet 2018 (18% Protein)	C57BL/6J	50	Total visceral adipose mass (g)/ body mass (g)	Adipose Tissue Weight
	8-week subchronic	Teklad Global Diet 2018 (18% Protein)	C57BL/6J	50	Perirenal adipose mass (g) / body mass (g)	Adipose Tissue Weight
	8-week subchronic	Teklad Global Diet 2018 (18% Protein)	C57BL/6J	50	Perigonadal adipose tissue mass (g) / body mass (g)	Adipose Tissue Weight
	8-week subchronic	Teklad Global Diet 2018 (18% Protein)	C57BL/6J	50	Mesenteric adipose mass (g) / body mass (g)	Adipose Tissue Weight
	8-week subchronic	Teklad Global Diet 2018 (18% Protein)	C57BL/6J	50	Pancreas mass (g)	Pancreas Weight

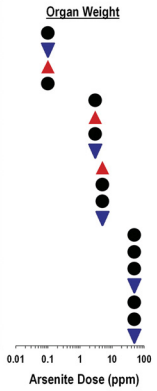

D.

Reference	Study Type	Diet	Species of mice	Dose (ppm)	Reported Endpoint	Consolidated Endpoint
Adebayo et al. 2015	5-week subchronic	AIN76A (21.5% Protein)	C57BL/6J	0.1	Body Weight	Body Weight
Ditzel et al. 2016	In utero (ED5) + 13-week chronic	TestDiet Western Diet (40.1% Fat)	Swiss Webster	0.1	Body Weight	Body Weight
	13-week chronic	TestDiet Western Diet (40.1% Fat)	Swiss Webster	0.1	Body Weight	Body Weight
Liu et al. 2014	16-week chronic	Standard chow (20% Protein)	C57BLKS/J db/m	3	Body Weight	Body Weight
	16-week chronic	Standard chow (20% Protein)	C57BKS/Lepr db/db	3	Body Weight	Body Weight
Lee et al. 2014	8-week subchronic	Standard chow diet	C57BL/6 db/db	10	Body weight	Body weight
Bae et al 2019	9-day subchronic	Standard chow diet (16% protein)	C57BL/6	5	Body weight	Body Weight
	9-day subchronic	Standard chow diet (16% protein)	C57BL/6	10	Body weight	Body Weight
Song et al. 2017	18-week chronic	Standard chow (20% Protein)	C57BL/6J	5	Body Weight	Body Weight
	18-week chronic	Standard chow (20% Protein)	C57BL/6J	50	Body Weight	Body Weight
Paul et al. 2007	8-week subchronic	Lab Diet 5058 (21.8% Protein)	C57BL/6J	25	Body Weight	Body Weight
	8-week subchronic	Lab Diet 5058 (21.8% Protein)	C57BL/6J	50	Body Weight	Body Weight
Kirkley et al. 2017	8-week subchronic	Teklad Global Diet 2018 (18% Protein)	C57BL/6J	50	Body Weight	Body Weight
Zuo et al. 2019	17-week chronic	Chow diet (Jiangsu Xietong Organism, Co)	C57BL/6J	5	Body Weight	Body Weight
	17-week chronic	Chow diet (Jiangsu Xietong Organism, Co)	C57BL/6J	20	Body Weight	Body Weight

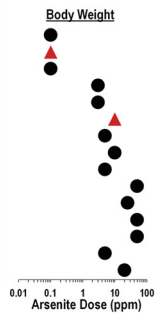

Figure 3. Graphical representation of the direction of the associations between oral exposure to arsenite and (A) insulin resistance, (B) impaired glucose tolerance, (C) organ weight, and (D) body weight, obtained from *in vivo* studies. Note: BW, body weight; GTT, glucose tolerance test; HOMA-IR, homeostatic model assessment for insulin resistance; ITT, insulin tolerance test; WAT, white adipose tissue. Upward-pointing red triangle, significantly higher outcome; downward-pointing blue triangle, significantly lower outcome; black circle, no statistical effect.

(Rodríguez et al. 2016). The brain has an obligate glucose requirement and therefore is especially vulnerable to impairments to glucose transporters (GLUT1 and GLUT3) required for glucose to cross the blood–brain barrier and be delivered to neurons (Rodríguez et al. 2016). Recent findings reported male C57BL/6J mice exposed to 50 ppm for 1 month experienced a decrease in GLUT1 and GLUT3 mRNA levels in the brain, despite a lack of significant change of serum glucose concentrations (Rodríguez et al. 2016). Interestingly, arsenite administration significantly increased insulin receptor expression in the hippocampus (Rodríguez et al.

A.

Reference	Exposure	Cell Type	Species, Tissue	Dose (μM)	Endpoint	Consolidated Endpoint
Hong and Bain et al. 2012	12, 24, 36, 48 days	C2C12 cells	Mouse, myoblast	0.02	Differentiation (IGF1 expression)	Differentiation
Beezhold et al. 2017	24 or 48 hours	Primary hMSCs	Human, stem cells	1	CYCLIND1 (G1 phase progression)*	Differentiation
Garciafigueroa et al. 2013	24, 48, or 72 hours	Primary hMSCs	Human, stem cells	1	PERILIPIN	Adipogenesis
	24, 48, or 72 hours	Primary hMSCs	Human, stem cells	1	Glycerol release (Lipolysis)	Anti-Adipogenesis
Xue et al. 2011	7 days	3T3-L1 cells	Mouse, fibroblast	0.25, 0.5, 1, 2	PPARG1 mRNA	Adipogenesis
	7 days	3T3-L1 cells	Mouse, fibroblast	0.25, 0.5, 1, 2	PPARG2 mRNA	Adipogenesis
	7 days	3T3-L1 cells	Mouse, fibroblast	0.25, 0.5, 1, 2	C/EBP-α	Adipogenesis
Klei et al. 2012	11 days	hMSCs	Human, stem cells	0.1, 0.25, 0.5, 1, 2.5	C/EBP-α	Adipogenesis
	12 days	Primary SVCs	Mouse, epididymal WAT	0.5, 2.5	PPARG (pg/mL product)	Adipogenesis
Yadav et al. 2012	21 days	hMSCs	Human, stem cells	0.2, 2, 4	C/EBP- α and β	Adipogenesis
	21 days	hMSCs	Human, stem cells	0.2, 2, 4	PPARG mRNA	Adipogenesis
	21 days	hMSCs	Human, stem cells	0.2, 2, 4	WNT3A	Anti-Adipogenesis
Hou et al. 2013	4-5 days	ADSVFCs, ADSCs	Mouse/Human, fibroblast	5	PPARG1 mRNA	Adipogenesis
	4-5 days	ADSVFCs, ADSCs	Mouse/Human, fibroblast	5	PPARG2 mRNA	Adipogenesis
	4-5 days	3T3-L1 cells	Mouse, pre-adipocytes	5	PPARG1 mRNA	Adipogenesis
Trouba et al. 2000	7-10 days	C3H 10T1/2 cells	Mouse, fibroblast	0.1, 0.3, 1, 3, 6	Terminal differentiation	Differentiation
Wauson et al. 2002	2 months	C3H 10T1/2 cells	Mouse, fibroblast	6	Adipogenesis	Adipogenesis
Bae et al 2019	6 days	HIB1B brown preadipocytes	Mouse, adipose	1, 2.5, 5, 10	Differentiation (PPARg)	Differentiation

*Under normal settings et al. cyclin D1 levels increase and then significantly decrease during proliferation and adipogenesis

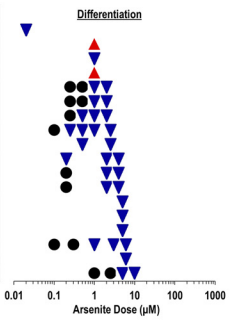

B.

Reference	Exposure	Cell Type	Species, Tissue	Dose (μM)	Endpoint	Consolidated Endpoints
Fu et al. 2010	96 hours	INS-1(832/13) cells	Rat, pancreas	0.05, 0.1,0.25, 0.5	NRF2	Inflammation (antioxidant)
	96 hours	INS-1(832/13) cells	Rat, pancreas	0.05, 0.1,0.25, 0.5	Intracellular glutathione	Inflammation (antioxidant)
	96 hours	INS-1(832/13) cells	Rat, pancreas	0.05, 0.1,0.25, 0.5	Peroxide-scavenging activity	Inflammation (antioxidant)
Druwe et al. 2012	24 or 48 hours	HepG2 cells	Human, liver	0.13, 0.67, 2	C-reactive protein (CRP)	Inflammation
	15 mins to 8 hours	HepG2 cells	Human, liver	0.13, 0.67	ROS	Inflammation
Yao et al. 2015	96 hours	INS-1 cells	Rat, pancreas	0.25, 0.5, 1	Thioredoxin reductase (TrxR) activity	Inflammation (antioxidant)
	96 hours	INS-1 cells	Rat, pancreas	0.25, 0.5, 1	ASK1 activity	Apoptosis
	96 hours	INS-1 cells	Rat, pancreas	0.25, 0.5, 1	CASPASE3 activity	Apoptosis
Díaz-Villaseñor et al. 2008	72 hours	RINm5F cells	Rat, pancreatic β-cells	0.5, 1, 2	CALPAIN10 activity	Apoptosis
	72 hours	RINm5F cells	Rat, pancreatic β-cells	0.5, 1, 2	15.6 mM glucose stimulated SNAP25 proteolysis	Apoptosis
Xue et al. 2011	7 days	3T3-L1 cells	Mouse, fibroblast	0.25, 0.5, 1, 2	NRF2 mRNA	Inflammation (antioxidant)
	7 days	3T3-L1 cells	Mouse, fibroblast	0.25, 0.5, 1, 2	Basal intracellular GSH	Inflammation (antioxidant)
	7 days	3T3-L1 cells	Mouse, fibroblast	0.25, 0.5, 1, 2	NRF2 protein	Inflammation (antioxidant)
	7 days	3T3-L1 cells	Mouse, fibroblast	0.25, 0.5, 1, 2	Intracellular peroxide	Apoptosis
Padmaja Divya et al. 2015	2, 4, or 8 weeks	3T3-L1 cells	Mouse, fibroblast	0.5, 1, 2	SIRT3 (Mitochondrial deacetylase)	Metabolic regulation
	8 weeks	3T3-L1 cells	Mouse, fibroblast	2	Mitochondrial membrane potential	Metabolic regulation/Inflammation/Apoptosis
	8 weeks	3T3-L1 cells	Mouse, fibroblast	2	Intracellular superoxide anion radical generation	Inflammation/Apoptosis
	2, 4, or 8 weeks	C2C12	Mouse, myotubes	0.5, 1, 2	SIRT3 (Mitochondrial deacetylase)	Metabolic regulation
	8 weeks	C2C12	Mouse, myotubes	2	Mitochondrial membrane potential	Metabolic regulation/Inflammation/Apoptosis
	8 weeks	C2C12	Mouse, myotubes	2	Intracellular superoxide anion radical generation	Inflammation/Apoptosis
Wu et al. 2018	3,6, 12, 24 hours (significance at 6 and 24)	INS-1 cells	Rat, pancreas	4	ER stress (PERK)	Inflammation
	3,6, 12, 24 hours (significance at 12 and 24)	INS-1 cells	Rat, pancreas	4	Autophagic flux	Apoptosis
Hou et al. 2013	6 hours	3T3-L1 cells	Mouse, fibroblast	0.25, 0.5, 1, 2, 5, 10	CHOP10 mRNA	Inflammation/Apoptosis
Pan et al. 2014	12 hours	INS-1 cells	Rat, pancreas	2.5, 5, 10	Intracellular ROS	Inflammation
	24 hours	INS-1 cells	Rat, pancreas	2.5, 5, 10	Mitochondrial membrane potential	Metabolic regulation/Inflammation/Apoptosis
	48 hours	INS-1 cells	Rat, pancreas	2.5, 5, 10	Lysosomal membrane potential	Apoptosis
Hamann et al. 2014	24 hours	HepG2 cells	Human, liver	0.1, 0.3, 1, 3, 10	Relative selenoprotein (SelP) mRNA levels	Inflammation (antioxidant)
	1 hour	HepG2 cells	Human, liver	10, 30, 100, 300, 1000	Relative glutathione levels	Inflammation (antioxidant)
	24 hours	HepG2 cells	Human, liver	10, 30, 100, 300, 1000	GSH	Inflammation (antioxidant)

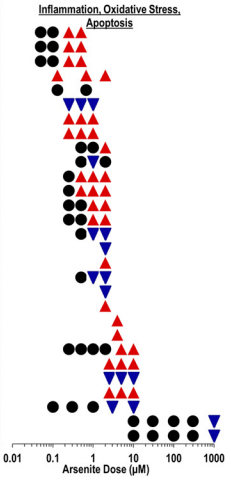

C.

Reference	Exposure	Cell Type	Species, Tissue	Dose (μM)	Endpoint	Consolidated Endpoints
Fu et al. 2010	96 hours	INS-1(832/13) cells	Rat, pancreas	0.05, 0.1,0.25, 0.5	Insulin mRNA	Insulin content
	96 hours	INS-1(832/13) cells	Rat, pancreas	0.05, 0.1,0.25, 0.5	Low (3 mM) GSIS	GSIS
	96 hours	INS-1(832/13) cells	Rat, pancreas	0.05, 0.1,0.25, 0.5	High (20 mM) GSIS	GSIS
	96 hours	INS-1(832/13) cells	Rat, pancreas	0.05, 0.1, 0.25, 0.5	Insulin mRNA	GSIS
	96 hours	INS-1(832/13) cells	Rat, pancreas	0.05, 0.1, 0.25, 0.5	Insulin content	GSIS
Díaz-Villaseñor et al. 2008	72 hours	RINm5F cells	Rat, pancreatic β-cells	0.5, 1, 2	Insulin mRNA	Insulin content
	72 hours	RINm5F cells	Rat, pancreatic β-cells	0.5, 1, 2	Low (5.6 mM) GSIS	GSIS
	72 hours	RINm5F cells	Rat, pancreatic β-cells	0.5, 1, 2	High (15.6 mM) GSIS	GSIS
Douillet et al. 2013	48 hours	Primary pancreatic islets	C57BL/6J mice, pancreas	0.1, 0.5, 1, 2	Low (2.5 mM) GSIS	GSIS
	48 hours	Primary pancreatic islets	C57BL/6J mice, pancreas	0.1, 0.5, 1, 2	High (16.7 mM) GSIS	GSIS
	48 hours	Primary pancreatic islets	C57BL/6J mice, pancreas	2	Secreted Islet insulin	Insulin responsiveness
	48 hours	Primary pancreatic islets	C57BL/6J mice, pancreas	2	Islet insulin content	Insulin content
	48 hours	Primary pancreatic islets	C57BL/6J mice, pancreas	2	Insulin mRNA	Insulin content
Díaz-Villaseñor et al. 2006	72 or 144 hours	Primary pancreatic β-cells	Wistar rats, pancreatic β-cells	1, 5	Insulin mRNA	Insulin content
	72 or 144 hours	Primary pancreatic β-cells	Wistar rats, pancreatic β-cells	1, 5	Low (5.6 mM) GSIS	GSIS
	72 or 144 hours	Primary pancreatic β-cells	Wistar rats, pancreatic β-cells	1, 5	High (15.6 mM) GSIS	GSIS
Hamann et al. 2014	24 hours	HepG2 cells	Human, liver	0.1, 0.3, 1, 3, 10	Relative G6Pase mRNA level	Insulin responsiveness
	24 hours	HepG2 cells	Human, liver	100, 300	Relative FOXO DNA binding activity	Insulin responsiveness
Dover et al. 2018	24 hours	INS1 832/13	Rat, pancreas	0.5, 1, 2	OCR(%)	GSIS

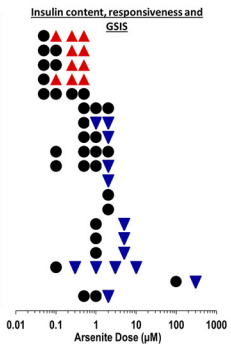

D.

Reference	Exposure	Cell Type	Species, Tissue	Dose (μM)	Endpoint	Consolidated Endpoints
Xue et al. 2011	7 days	3T3-L1 cells	Mouse, fibroblast	0.25, 0.5, 1, 2	GLUT4 mRNA	Glucose uptake
	7 days	3T3-L1 cells	Mouse, fibroblast	0.25, 0.5, 1, 2	AKT S473 phosphorylation	Glucose uptake
	4 or 7 days	3T3-L1 cells	Mouse, fibroblast	0.25, 0.5, 1, 2	Insulin stimulated (5 ng/mL) glucose uptake	ISGU
Zhang et al. 2017	4 hours	Primary hepatocytes	C57BL/6J mice, liver	0.5, 1, 2	Glycogen content	Glucose metabolism
	4 hours	Primary hepatocytes	C57BL/6J mice, liver	0.5, 1, 2	AKT Phosphorylation	ISGU
	4 hours	Primary hepatocytes	C57BL/6J mice, liver	0.5, 1, 2	Glycogen synthase (GS)	ISGU
	4 hours	Primary hepatocytes	C57BL/6J mice, liver	0.5, 1, 2	Glycosen phosphorylase (GP)	ISGU
	5 hours	Primary hepatocytes	C57BL/6J mice, liver	0.5, 1, 2	Free glucose content	Glucose metabolism
	6 hours	Primary hepatocytes	C57BL/6J mice, liver	0.5, 1, 2	Glycogen synthase activity	Glucose metabolism
	7 hours	Primary hepatocytes	C57BL/6J mice, liver	0.5, 1, 2	Relative glycogen phosphorylase activity	Glucose metabolism
Padmaja Divya et al. 2015	8 weeks	3T3-L1 cells	Mouse, fibroblast	0.5, 1, 2	Insulin stimulated (0.1 uM) glucose uptake	ISGU
	8 weeks	C2C12	Mouse, myotubes	0.5, 1, 2	Insulin stimulated (0.1 nM) glucose uptake	ISGU
	8 weeks	C2C12	Mouse, myotubes	0.5, 1, 2	GLUT4	ISGU
	8 weeks	3T3-L1	Mouse, fibroblasts	0.5, 1, 2	GLUT4	ISGU
Hamann et al. 2014	24 hours	HepG2	Human, liver	0.3, 0.1, 1, 3, 10	G6Pase	ISGU
	24 hours	HepG2	Human, liver	3,10	AKT	ISGU
	1 hour	HepG2	Human, liver	100, 300	FOXO1	ISGU
Walton et al. 2004	4 or 24 hours	3T3-L1 cells	Mouse, fibroblast	5, 10, 20, 100	Insulin stimulated (1 uM) glucose uptake	ISGU
	4 or 24 hours	3T3-L1 cells	Mouse, fibroblast	50	AKT phosphorylation	ISGU
	4 or 24 hours	3T3-L1 cells	Mouse, fibroblast	20, 100	Basal glucose uptake	Glucose uptake
Bazuine et al. 2003	30 minutes	3T3-L1 cells	Mouse, fibroblast	500	GLUT1 translocation to plasma membrane	Glucose uptake
	30 minutes	3T3-L1 cells	Mouse, fibroblast	500	GLUT4 translocation to plasma membrane	Glucose uptake

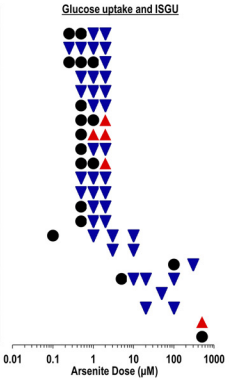

Figure 4. Graphical representation of the direction of the associations between arsenite treatment and (A) differentiation, (B) oxidative stress and inflammation, (C) glucose-stimulated insulin secretion (GSIS), and (D) insulin-stimulated glucose uptake (ISGU), obtained from *in vitro* studies. Note: AKT, protein kinase B; ASK1, apoptosis signal-regulating kinase 1; C/EBP, CCAAT-enhancer-binding protein α and β; CHOP10, CCAAT-enhancer-binding protein homologous protein-10; FOXO, forkhead box transcription factor; GLUT, glucose transporter type; G6Pase, glucose 6-phosphatase; NRF2, nuclear factor-erythroid 2-related factor 2; OCR, oxygen consumption rate; PERK, eukaryotic translation initiation factor 2 alpha kinase 3; PPAR, peroxisome proliferator–activated receptor; ROS, reactive oxygen species; SIRT, sirtuin 3. Upward-pointing red triangle, significantly higher outcome; downward-pointing blue triangle, significantly lower outcome; black circle, no statistical effect.

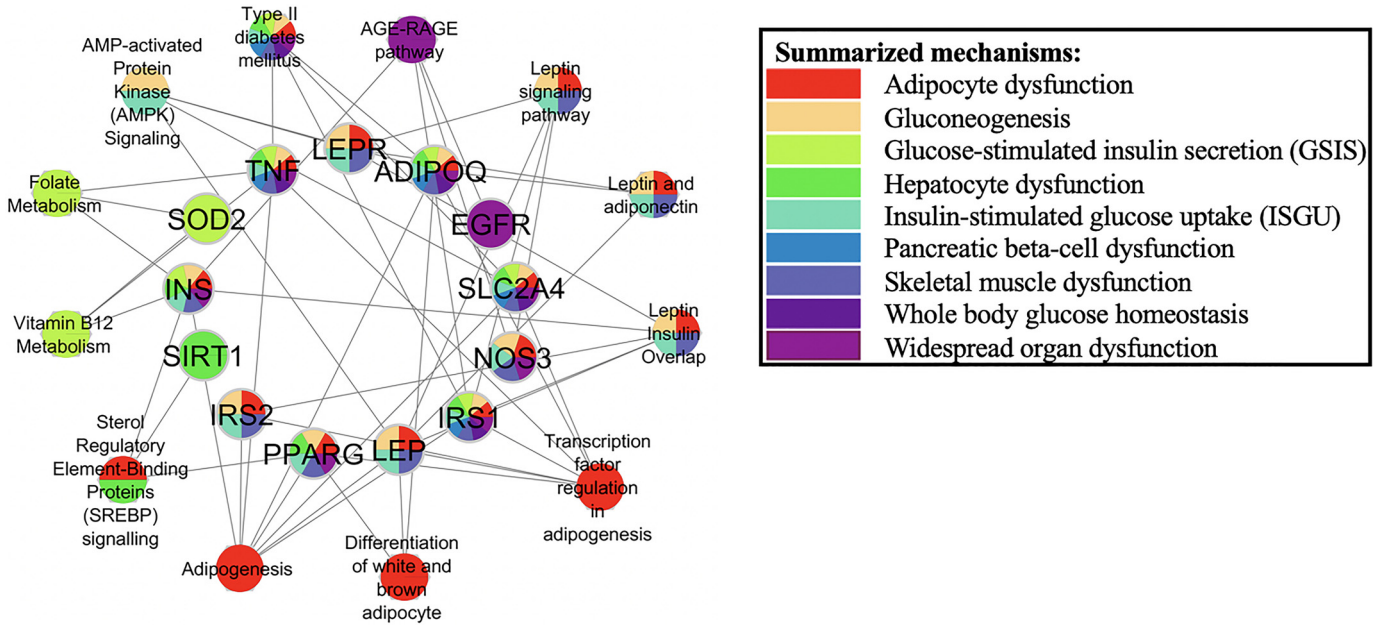

Figure 5. A network of biological pathways and connected genes that were in common between arsenic (iAs3 +), insulin resistance, and type 2 diabetes (T2D) as found using publicly available gene association data from the Comparative Toxicogenomics Database (CTD). A network of 12 biological pathways and 13 connected genes that were in common between iAs3 +) exposure, insulin resistance (IR), and type 2 diabetes (T2D) as found using publicly available gene association data from the CTD. Gene set enrichment analysis (GSEA) was performed with the Cytoscape app ClueGO using the WikiPathways repository (containing 418 human pathways and 5,866 human genes) (WikiPathways 2018). Only pathways containing more than three genes or comprising 4% of the total number of genes in a pathway are depicted in the network. Following GSEA, pathways and genes were assigned to any of the nine summarized phenotypes as described in the paper. The colored pie charts, depicted in the network nodes, represent the different phenotypes associated with that specific pathway or gene. For the label of the gene node, the official HUGO Gene Nomenclature Committee (HGNC)–approved human gene name is used. The label of the pathway node contains the WikiPathway name of the pathway. Note: ADIPOQ, Adiponectin, C1Q And Collagen Domain Containing; EGFR, Epidermal Growth Factor Receptor; INS, Insulin; IRS1, Insulin Receptor Substrate 1; IRS2, Insulin Receptor Substrate 2; LEP, Leptin; LEPR, Leptin Receptor; NOS3, Nitric Oxide Synthase 3; PPARG, Peroxisome Proliferator Activated Receptor Gamma; SIRT1, Sirtuin 1; SLC2A4, Solute Carrier Family 2 Member 4; SOD2, Superoxide Dismutase 2; TNF, Tumor Necrosis Factor.

2016). However, it is unclear whether the change of glucose tolerance was due to the reduction of GLUT1 and GLUT3 expression in the hippocampus (Rodríguez et al. 2016).

A recent study showed impaired brown adipose tissue activity (BAT) in female C57BL/6J mice exposed to 5 or 20 ppm arsenic for 17 wk (Zuo et al. 2019). While these mice experienced no changes in body weight, BAT mass was significantly elevated in the 5-ppm exposure group, with significantly increased adipocyte droplets based on histopathological analysis (Zuo et al. 2019). Moreover, insulin levels were significantly elevated at both concentrations of exposure, with a significant decrease in genes involved in thermogenesis [uncoupling protein 1 (UCP1) and PGC1α] and mitochondrial respiratory chain activity [Cytochrome C Oxidase Subunit IV (COXIV) and NADH:Ubiquinone Oxidoreductase Subunit S4 (NDUFS4)] (Zuo et al. 2019). Another recent study corroborated Zuo et al. 2019's findings in male C57BL/6J mice exposed to 5 and 10 ppm arsenic for 9 d (Bae et al. 2019). Bae et al. (2019) reported arsenic accumulation in BAT, with a significant decrease in lipogenesis, autophagy, and thermogenesis (Bae et al. 2019). The authors also found arsenite exposure to impair differentiation of HIB1B brown preadipocytes following a 6-d exposure to arsenite at 2.5-, 5-, and 10-μM concentrations (Bae et al. 2019). Both *in vivo* and *in vitro*, UCP1, PGC1, peroxisome proliferator–activated receptor gamma (PPARγ), and PR/SET Domain 16 (PRDM16) were all found to be significantly decreased (Bae et al. 2019).

Studies focused on arsenic's effects on ISGU have most frequently relied on 3T3-L1 adipocytes to demonstrate impaired effects at both high and low exposures (Figure 4). Skeletal muscle, however, is primarily responsible for the majority of insulin-dependent glucose utilization in the body (DeFronzo 2009). The only cell culture model used to study the effects of arsenic on myotubes has been C2C12 myotubes, and arsenite exposure was shown to impair C2C12 differentiation *in vitro* (Hong and Bain 2012). Future studies should focus on the effects of arsenic on primary myotubes isolated from both rodents and humans. A recent study reported impaired skeletal muscle function, myofiber hypertrophy, mitochondrial myopathy, and altered oxygen consumption after 5 wk of arsenite exposure (100 ppb) in 5- to 6-wk-old C57BL/6NTac male mice (Ambrosio et al. 2014). While these *in vivo* findings support the evidence found in cultured myotubes (C2C12), additional studies will provide valuable insight regarding arsenic toxicity.

The network analyses performed in this review support experimental findings and highlight genes involved in insulin resistance and metabolic disorders. These include insulin, insulin receptor substrate 1 and 2, and heme oxygenase 1 (Figure 2). Arsenic's effects on alterations in gene expression associated with these pathways can have deleterious effects on ISGU and whole-body glucose homeostasis, as demonstrated in Figures 3 and 4.

Hepatic Glucose Metabolism and Insulin Signaling

The liver is a key target tissue for arsenic-induced insulin resistance due to its role in both arsenic metabolism and glucose production. Insulin suppresses hepatic gluconeogenesis and glycogenolysis, which are impaired in T2D (Basu et al. 2004). Gluconeogenesis is mainly regulated by the modulation of the transcription of rate-controlling enzymes in the pathway, such as phosphoenolpyruvate carboxykinase (PCK1) and the catalytic subunit of glucose 6 phosphatase (G6PC) (Pilkis and Granner 1992). Insulin inhibits the transcription of both PCK1 and G6PC. To inhibit glycogenolysis,

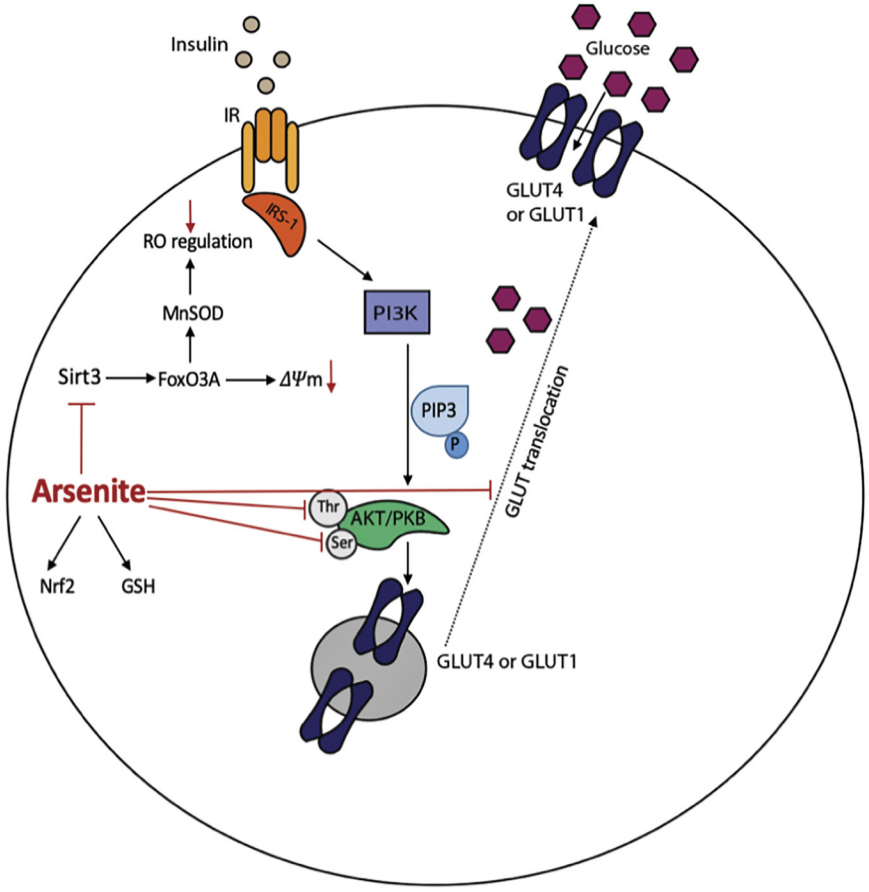

Figure 6. Arsenite impairs insulin-stimulated glucose uptake (ISGU) in adipocytes and myotubes. Arsenite has been shown to down-regulate AKT and glucose transporter translocation to the plasma membrane in both adipocytes and myotubes (Walton et al. 2004; Xue et al. 2011). Arsenite also up-regulates antioxidant defenses such as NRF2 and GSH, inhibiting endogenous ROS involved in ISGU (Xue et al. 2011; Xu et al. 2012). *In vitro*, arsenite has been shown to inhibit SIRT3–FOXO3A signaling to reduce mitochondrial activity and impair ISGU (Padmaja Divya et al. 2015). Note: AKT/PKB, protein kinase B; FOXO3A, forkhead box O3; GLUT, glucose transporter type; GSH, glutathione; IR, insulin receptor; IRS1, insulin receptor substrate-1; NRF2, nuclear factor-erythroid 2-related factor 2; PIP3, phosphatidylinositol 3,4,5-triphosphate; PI3K, phosphoinositide 3-kinase; ROS, reactive oxygen species; SIRT3, sirtuin 3.

insulin activates protein phosphatase 1 that inhibits glycogen phosphorylase (GP), which catalyzes the rate-limiting step of glycogenolysis (Petersen et al. 2017).

Identified studies showed that treating C57BLKS/J$^{db/m}$ and C57BLKS/J$^{db/db}$ male mice with 3 ppm arsenite for 16 wk increased PCK1 overexpression (Liu et al. 2014). A rise in protein levels of Na^+K^+-ATPase was observed in the liver of arsenite-treated mice (Liu et al. 2014). Arsenite treatment did not affect fasting blood glucose (FBG) levels in C57BLKS/J$^{db/m}$ mice. However, arsenite treatment elevated fasting glucose levels in C57BLKS/J$^{db/db}$ mice (Liu et al. 2014). The rates of gluconeogenesis and glycogenolysis were not measured in this study (Liu et al. 2014). A similar study in C57BL/6 *db/db* obese mice exposed to 10 ppm arsenite for 8 wk found a significant decrease in phosphoenolpyruvate carboxykinase (PEPCK) and G6PC RNA in the livers of exposed mice (Lee et al. 2014). Thus, the exact mechanism governing the elevation of FBG is unclear in arsenic-exposed diabetic mice.

A recent study reported a dose-dependent decrease in glycogen content in mouse primary hepatocytes treated with low-dose (0.5–2 μM) arsenite for 4 h (Zhang et al. 2017). Exposure to arsenite resulted in a dose-dependent reduction in insulin-dependent activation of glycogen synthase (GS), the rate-controlling enzyme in glycogenesis, and activation of GP, the rate-controlling enzyme in glycogenolysis (Zhang et al. 2017). Arsenite treatment for 4 h also inhibited insulin-stimulated AKT phosphorylation at serines 308 and 473, characteristic of AKT activity (Zhang et al. 2017). In contrast, the activity of glycogen synthase kinase 3, a downstream effector of AKT, was not affected by exposure to arsenite (Zhang et al. 2017).

The dose and duration of arsenic treatment *in vitro* can be a critical factor in identifying targets of arsenic toxicity relevant to human exposures. A study found that chronic treatment in mice (8 wk) with high arsenite exposure (150 ppm) resulted in hepatic damage with observed tissue necrosis and significantly elevated serum glutamate–pyruvate transaminase (Noman et al. 2015). HepG2 human hepatoma cells have been used as a model to study both the long- and short-term effects of arsenite on insulin signaling. While a 1-h exposure to arsenite at concentrations up to 1 mM did not alter cell viability, the authors observed a decrease in GSH (Hamann et al. 2014). Conversely, cell viability was greatly reduced after 24 h of arsenite treatment (Hamann et al. 2014). HepG2 cells treated with 3 or 10 μM of arsenite for 24 h attenuated insulin's ability to activate AKT (Hamann et al. 2014). The phosphorylation of IR by insulin was reduced with exposure to 10 μM but not 3 μM of arsenite (Hamann et al. 2014). Similar to findings from murine primary hepatocytes, arsenite treatment did not induce changes in GSK3 activity (Hamann et al. 2014). The phosphorylation of another insulin-induced downstream effector of AKT, FOXO1, was also not affected by arsenite treatment (Hamann et al. 2014). Surprisingly, while insulin inhibits the expression of G6PC in healthy individuals (Hutton and O'Brien

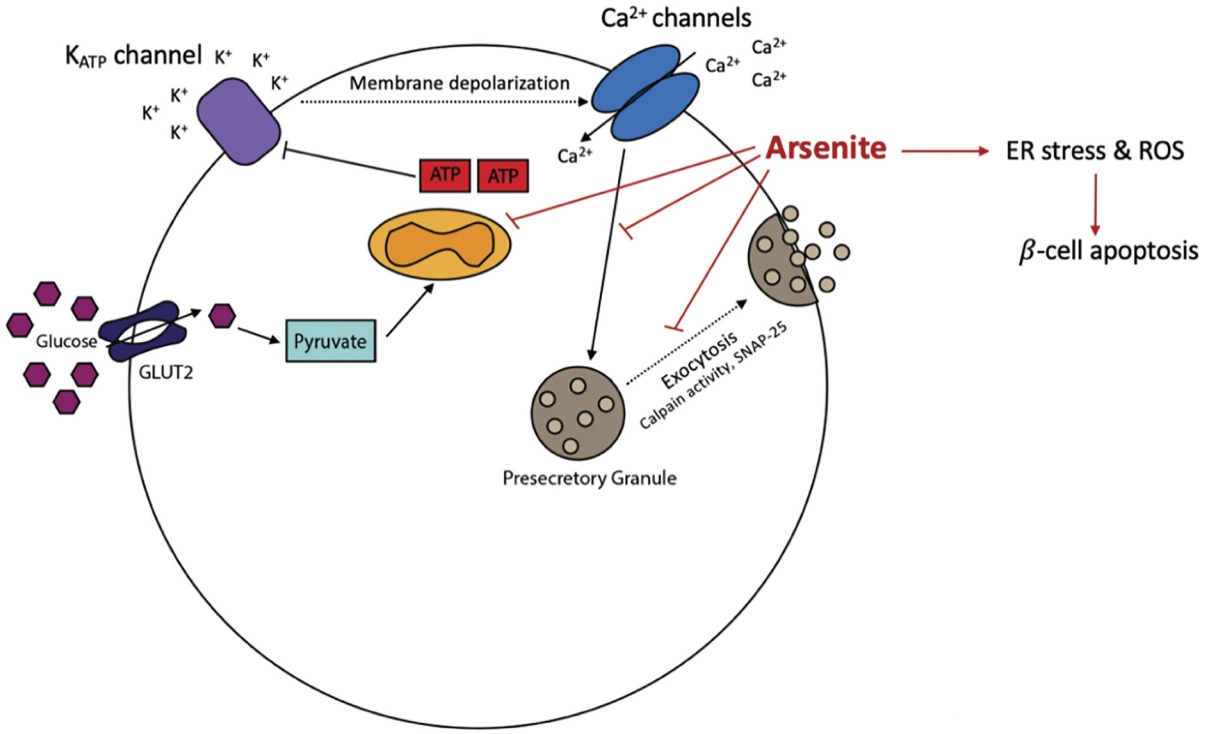

Figure 7. Arsenite disrupts glucose-stimulated insulin secretion (GSIS) in pancreatic β cells. Arsenite treatment *in vitro* has been reported to decrease calpain activity, measured as SNAP25 proteolysis. SNAP25 and CALPAIN10 are both needed to fuse insulin presecretory granules with the plasma membrane for insulin secretion. At higher doses, arenite has also been shown to increase ER oxidative stress, which can lead to apoptosis of pancreatic β cells due to the tissue's low abundance of antioxidants (Wu et al. 2018; Pan et al. 2016; Yao et al. 2015). Note: Ca^{2+}, calcium; ER, endoplasmic reticulum; GLUT, glucose transporters; K, potassium; ROS, reactive oxygen species; SNAP25, synaptosome-associated protein 25.

2009), 24 h of arsenite treatment (1, 3, and 10 μM) also significantly suppressed G6PC expression in Hep2G cells (Hamann et al. 2014). The combinatorial effect of insulin and arsenite on G6PC expression, however, was not examined. For short-term exposures, HepG2 cells treated with 100 and 300 μM of arsenite for 1 h induced both AKT and FOXO1 phosphorylation (Hamann et al. 2014). Thus, in contrast to the inhibitory effect on insulin action observed after 24 h arsenite treatment, 1 h of arsenite treatment mimicked insulin-like signaling (Hamann et al. 2014). These findings highlight how the duration of arsenite exposure *in vitro* may have significant implications on our interpretation of epidemiologic findings.

Additional studies assessing arsenic's effects on hepatic glucose regulation are needed. While the current literature is sparse, studies suggest that low-dose arsenite treatment of more than 4 h may alter insulin's anabolic activity in hepatocytes *in vitro*. The network analyses highlight genes involved in hepatic lipid metabolism and inflammation, such as SIRT1 and sterol regulatory element-binding protein (SREBP) (Figure 5). The chemical's pronounced effects on liver function, hepatic steatosis, and injury have also been widely reported in murine models (Ditzel et al. 2016; Shi et al. 2014; Noman et al. 2015). However, whether arsenic exposure modulates gluconeogenesis and glycogenolysis *in vivo* remains unexplored.

Glucose-Stimulated Insulin Secretion and β-cell Function

Pancreatic β cells respond to elevated plasma glucose levels to secrete insulin, which, in turn, stimulates glucose utilization in skeletal muscle and white adipose tissue. This process allows mammals to maintain plasma glucose levels in a narrow range of homeostasis. An identified study showed that treating 8-wk-old C57BL/6J male mice with 50 ppm arsenite for 8 wk resulted in impaired glucose tolerance (Kirkley et al. 2017). Whereas no differences in peripheral insulin sensitivity were observed between groups, arsenic-treated mice experienced a reduction in glucose-stimulated insulin secretion (GSIS) compared to controls (Kirkley et al. 2017). High-dose exposure did not affect pancreatic β-cell mass or structure, suggesting that arsenite affects β-cell function (Kirkley et al. 2017). The ability of arsenic to induce ROS and free radicals has been previously reported in human fibroblast cells (Hu et al. 2002). The pancreas has low antioxidant capabilities and therefore may be especially vulnerable to arsenic-induced oxidative stress (Keane et al. 2015). INS-1832/13 cells treated with low-dose arsenite for 24 h decreased both GSIS and mitochondrial respiration in a dose-dependent manner (Dover et al. 2018). Low levels (0.25 and 0.5 μM) of arsenite treatment for 96 h dampened glucose-induced insulin secretion in INS-1 832/13 rat pancreatic β cells by activating NRF2 activity, which activates the transcription of genes involved in antioxidant defenses. Once activated, these genes decreased endogenous peroxide production necessary for adequate glucose-induced insulin secretion (Fu et al. 2010). Arsenite treatment did not affect insulin gene expression in this report, which suggests that the secretion of insulin, but not its synthesis, is the target of arsenic toxicity (Fu et al. 2010). Additional studies report similar findings, as arsenic was shown to attenuate GSIS without affecting insulin synthesis in pancreatic islets from mice (Douillet et al. 2013) and in RINm5F cells (Díaz-Villaseñor et al. 2008) (Figure 3). Another report, however, shows that high levels of sodium arsenite treatment (5 μM) for 72 and 144 h in pancreatic β cells isolated from male Wistar rats resulted in significantly lower insulin gene expression (54 and 72%, respectively) (Díaz-Villaseñor et al. 2006). Both dose and duration of treatment requires careful consideration, as 5 μM significantly decreased

pancreatic β-cell viability after 144 h but not 72 h (Díaz-Villaseñor et al. 2006).

Arsenite may reduce GSIS by interfering with calcium-mediated signaling required for insulin secretory granule exocytosis. Calpains are calcium-sensing proteases that activate proteins such as synaptosome-associated protein 25 (SNAP25), which is involved in insulin secretory vesicle exocytosis (Marshall et al. 2005). SNAP25 and CALPAIN10 both mediate the fusion of insulin granules with the plasma membrane (Marshall et al. 2005). While low-dose (0.5–1 μM) arsenite treatment of RINm5F rat pancreatic β cells for 72 h did not decrease CAPLAIN10 activity with either basal (5.6 mM) or elevated (15.6 mM) glucose stimulation, CALPAIN10 activity was significantly increased at 2 μM arsenite treatment during both basal and elevated glucose levels (Díaz-Villaseñor et al. 2008). Treatment with 1 μM arsenite during insulin-stimulated glucose secretion *in vitro* lowered calpain activity, measured as SNAP-25 proteolysis (Díaz-Villaseñor et al. 2008). While CALPAIN10 activity was significantly increased only after 2 μM arsenite treatment, its activity was trending upward starting at 0.5 μM (Díaz-Villaseñor et al. 2008). Arsenite concentrations at 1, 2, and 5 μM all significantly reduced cell viability (Díaz-Villaseñor et al. 2008).

Endoplasmic reticulum (ER) stress is an additional mechanism involved in impaired GSIS (Hasnain et al. 2016). Sodium arsenite (4 μM) treatment in INS-1 cells for 3, 6, 12, and 24 h activated ER stress, as measured by eukaryotic translation initiation factor 2 alpha kinase 3 (PERK) activity (Wu et al. 2018). Treating arsenite-treated pancreatic islets with PERK inhibitor restored the capacity of GSIS (Wu et al. 2018). This finding suggests arsenite-induced ER stress can suppress GSIS (Figure 4). The induction of ER stress and autophagy is likely to be cell autonomous, as treating INS-1 rat insulinoma cells with arsenite (4 μM) for 6 h potentiated PERK activity and altered the expression of autophagy makers (Wu et al. 2018).

Oxidative stress induced by arsenite treatment in β cells has been shown to induce apoptosis. INS-1 832/13 pancreatic β cells treated with sodium arsenite (2.5–10 μM) exhibited increased intracellular ROS levels and apoptosis (Pan et al. 2013). Arsenite exposure also significantly reduced mitochondrial membrane potential and lysosomal membrane composition (Pan et al. 2013). Low-dose arsenite (0.25–1 μM) exposure in INS-1 832/13 pancreatic β cells for 96 h decreased cell viability and thioredoxin reductase (TRX) activity in a dose-dependent manner (Yao et al. 2015). TRX is an enzyme that protects cells from oxidative damage and also associates with and suppresses the activity of apoptosis signal-regulating kinase 1 (ASK1), a protein kinase involved in apoptosis (Soga et al. 2012). Indeed, the levels of ASK1 protein were increased in cell culture media upon arsenite treatment (Yao et al. 2015). Moreover, reducing ASK1 expression by RNA interference attenuated arsenite-induced cytotoxicity (Yao et al. 2015). Thus, arsenic reduced TRX activity, which, in turn, activated ASK1 to induce apoptosis in INS-1 cells. Most significantly, although NRF2 activation reduced GSIS as previously described, NRF2-induced antioxidant response has been shown to be involved in protecting pancreatic β cells from arsenic-induced cellular damage. Both NRF2-knockdown MIN6 pancreatic β cells and pancreatic islets isolated from NRF2-knockout mice experienced increased cytotoxicity upon 2–6 h of arsenite (2–10 μM) treatment (Yang et al. 2012). MIN6 NRF1 knockdown cells also had decreased antioxidant capabilities (Cui et al. 2017). *In vitro* findings showed arsenite treatment decreased cell viability (1–20 μM for 24 h) and enhanced expression of genes involved in arsenic metabolism (Cui et al. 2017). These results further corroborate the role of arsenite-induced oxidative stress in pancreatic β-cell apoptosis. HepG2 cells treated with low-dose arsenite (0.13–2 μM) for 24 h experienced a significant rise in C-reactive protein (CRP), which is secreted in response to increased inflammation (Druwe et al. 2012). These experimental findings are consistent with the increased levels of CRP observed in FVB female mice treated with 100 ppb arsenite via drinking water for 22 wk (Druwe et al. 2012). Another study found 16 wk of arsenite (3 ppm) exposure increased inflammation, ROS, and vacuole formation in pancreatic islet of db/m mice and further exacerbated these conditions in db/db mice (Liu et al. 2014).

In vivo studies that assess the effect of arsenic on the pancreas were conducted by exposing rodents at parts-per-million levels for a duration of at least 8 wk. Several of these studies showed that arsenic treatment increased pancreatic damage, which is in agreement with *in vitro* studies that report exposures starting at 1 μM to induce apoptosis. Most studies (Díaz-Villaseñor et al. 2008; Douillet et al. 2013; Díaz-Villaseñor et al. 2006; Hamann et al. 2014) that treat with arsenic levels >1 μM report a reduction in GSIS, which supports dose-specific effects on glucose homeostasis (Figure 4). Studies suggest that lower dose and/or shorter exposure duration (Fu et al. 2010; Yao et al. 2015; Wu et al. 2018; Pan et al. 2013) have the potential to induce pancreatic β-cell inflammation and decrease pancreatic tissue weight (Liu et al. 2014; Kirkley et al. 2017). Discrepancies in experimental findings reported across animal studies may also be due to different susceptibilities across animal strains and species (Gentry et al. 2004). Several mechanisms were identified as mediating arsenic-induced β-cell apoptosis, including up-regulated oxidative and ER stress (Figure 4). Interestingly, arsenic activation of NRF2 may inhibit endogenous ROS necessary for glucose uptake and insulin secretion (Xu et al. 2012). However, the activation of NRF2 was also shown to protect β cells from apoptosis (Masuda et al. 2015) and therefore has multiple implications in maintaining glucose homeostasis at various arsenic exposure concentrations. The network analyses performed reveal five genes associated with oxidative stress and inflammatory responses, including complement 3 (C3), tumor necrosis factor (TNF), nitric oxide synthase 3 (NOS3), heme oxygenase 1 (HMOX1), and superoxide dismutase 2 (SOD2) (Figure 5). Further investigation of these mechanisms at chronic low doses relevant to human exposures is necessary going forward (Hectors et al. 2011).

Adipose Tissue Function

White adipose tissue is the primary organ responsible for the storage of lipids in the form of triglycerides. Increased lipolysis contributes to ectopic lipid deposition in target tissues involved in glucose metabolism, such as the liver and skeletal muscle (Rosen and Spiegelman 2006). Ectopic lipid deposition is one of the major mechanisms of insulin resistance (Rosen and Spiegelman 2006). Thus, both excess storage of lipids in white adipose tissue, such as obesity and lipodystrophy, have significant effects on insulin sensitivity and glucose homeostasis (Rosen and MacDougald 2006; Rosen and Spiegelman 2006). Adipose tissue is also an endocrine organ that secretes various adipokines to modulate metabolic functions (Coelho et al. 2013; Kershaw and Flier 2004). Both *in vivo* and *in vitro* studies have found arsenic treatment to modulate adipocyte function and differentiation (Figures 2 and 3, respectively). Exposure to arsenite (5 or 50 ppm) in 4-wk-old C57BL/6J male mice for 18 wk significantly decreased serum adiponectin levels (Song et al. 2017), a key adipokine in insulin sensitivity (Rosen and Spiegelman 2006; Ye and Scherer 2013). However, it remains unclear whether the reduction of plasma adiponectin levels contributes to arsenic's effects.

Most of the *in vivo* studies of chronic arsenite exposure found in our search showed no significant differences in weight gain or overall body mass (Figure 3) (Adebayo et al. 2015; Ambrosio et al. 2014; Kirkley et al. 2017; Song et al. 2017). Treating 5- to 6-wk-old C57BL/6J male mice with 100 ppb arsenite for 5 wk induced

lipid mobilization that resulted in elevated ectopic accumulation of lipids in skeletal muscle (Garciafigueroa et al. 2013). Treating adipocytes differentiated from human mesenchymal stem cells (hMSCs) with 1 μM arsenite for 72 h increased glycerol release, an indicator of the lipolytic activity in adipocytes (Garciafigueroa et al. 2013). Interestingly, arsenite treatment also resulted in lower expression of PERILIPIN1, a lipid droplet protein found in adipocytes (Garciafigueroa et al. 2013). These responses were reduced by pertussis toxin, an inhibitor of Gi-α subunit of heterotrimeric G protein. Indeed, antagonizing Gi-coupled endothelin-1 type A receptor attenuated arsenite's lipolytic response, whereas antagonizing endothelin-1 type B receptor decreased the ability of arsenite to suppress PERILIPIN1 expression (Garciafigueroa et al. 2013). These results suggest that arsenic modulates PERILIPIN1 expression and lipolysis through different mechanisms (Figure 4). PERILIPIN1 does, however, play an important role in the regulation of lipolysis in adipocytes (Sztalryd and Brasaemle 2017). PERILIPIN1 associates with and inhibits adipocyte triglyceride lipase (ATGL), an enzyme that hydrolyzes triacylglycerol to diacylglycerol. Upon the induction of protein kinase A (PKA) signaling by norepinephrine, PERILIPIN1 is phosphorylated by PKA, which prompts its dissociation from ATGL. Phosphorylated PERILIPIN1 subsequently recruits phosphorylated hormone-sensitive lipase, which hydrolyzes diacylglycerol to monoacylglycerol. This process enhances lipolysis in adipocytes. Thus, reducing the expression of PERILIPIN1 will result in the augmentation of basal lipolysis, yet also attenuate norepinephrine- and cyclic adenosine monophosphate cAMP-induced lipolysis.

Adipocyte number (hyperplasia) and size (hypertrophy) are important features of white adipose tissue. Five-week arsenite exposure (100 ppb) *in vivo* was shown to reduce adipocyte numbers in white adipose tissue (Garciafigueroa et al. 2013). These results suggest arsenite treatment impairs adipogenesis (Figure 4). Pertussis toxin and antagonists of endothelin-1 type A and B receptors decreased arsenite's ability to inhibit hMSCs differentiation into adipocytes (Klei et al. 2012). Moreover, reduced expression of endothelin-1 type A and B receptors in preadipocytes attenuated arsenite-inhibited adipogenesis (Klei et al. 2012). These results suggest that the ability of arsenite to inhibit adipogenesis, like its effect on lipolysis, requires, at least in part, endothelin-1 type A and B receptors.

A multitude of studies have observed the suppressive effect of arsenite on adipogenesis (Figure 4) (Ceja-Galicia et al. 2017; Hou 2013; Trouba et al. 2000; Wauson et al. 2002). Arsenite (0.2–4 μM) treatment of hMSCs impaired differentiation to adipocytes (Yadav et al. 2013). Perhaps unsurprisingly, the expression of transcription factors involved in adipogenesis, such as PPARγ and CCAAT-enhancer binding protein α and β (C/EBPα and C/EBPβ), were also reduced, whereas the expression of adipogenic inhibitor Wnt family member 3A (Wnt3a) was increased (Yadav et al. 2013). Arsenite treatment in 3T3-L1 preadipocytes also suppressed differentiation to adipocytes (Hou et al. 2013). Arsenite treatment resulted in higher levels of CCAAT-enhancer-binding protein homologous protein-10 (CHOP10), an ER stress response protein involved in the unfolded protein response (UPR) (Hou et al. 2013). CHOP10 is a negative regulator of C/EBPβ, which acts upstream of PPAR actors involved in adipogenesis, such as PPARγ and C/EBPα, in the transcriptional cascade regulating adipogenesis (Hou et al. 2013). C3H 10T1/2 preadipocytes exposed to sodium arsenite (6 mM) for 8 wk also experienced altered morphology and impaired differentiation (Trouba et al. 2000). Arsenite-treated human hMSCs (1 μM for 24 and 48 h) exhibited significantly altered function of noncoding microRNA involved in adipogenesis (Beezhold et al. 2017; Renu et al. 2018). Both culture adipocytes and primary hMSCs isolated from mice treated with arsenite *in vivo* (100–250 ppb) increased microRNA 29 (miR-29) and cyclin D1 (CCND1) expression, furthering cell growth rather than adipogenic differentiation (Beezhold et al. 2017).

Recent findings suggest low- and moderate-dose arsenite exposure induces lipolysis and impairs adipogenesis (Renu et al. 2018). Mechanistic studies indicate a dose-dependent inhibition of adipocyte differentiation, altering critical pro-adipogenic programming (Figure 4). Arsenic's effects in adipose tissue also manifest in increased ectopic lipid deposition in both the liver and skeletal muscle, which could contribute to the development of insulin resistance (Renu et al. 2018). Gene lists obtained from our network analyses complement findings in both *in vivo* and *in vitro* studies and support adipose tissue as a target of arsenic toxicity. Many of the genes highlighted in the network analyses (Figure 5) are directly involved in adipogenesis, altered energy storage, adipokine secretion, and ectopic lipid deposition, further supporting the experimental evidence reported. Figure 5 lists the pathways related to arsenic-induced insulin resistance and also depicts the interaction network of both these pathways and select genes identified.

Trivalent Arsenical Metabolites: $DMA^{III}+$ and $MMA^{III}+$

Since epidemiologic studies have reported the association of arsenic and T2D, the primary focus of laboratory research in the context of diabetes has relied on the parent compound as the chemical of exposure (Castriota et al. 2018; Farzan et al. 2017; Grau-Perez et al. 2017; Pan et al. 2013; Peng et al. 2015). Recent evidence, however, has shown trivalent arsenical species interfere with metabolic pathways responsible for glucose homeostasis. A dose-dependent decrease in mitochondrial respiration associated with GSIS in INS-1 832/13 pancreatic β cells was observed for both arsenite and $MMA^{III}+$ but not for $DMA^{III}+$ (Dover et al. 2018). $MMA^{III}+$ decreased GSIS in INS-1 cells after 24 h exposure at both 0.375 and 0.5 μM (Dover et al. 2018). There was, however, no significant decrease observed upon 24 h DMA exposure, even at the highest dose (Dover et al. 2018). This research highlights key differences in the effects of arsenical species on GSIS, warranting increased laboratory research on this pathway.

Four hours of exposure to arsenite and $MMA^{III}+$ concentrations as low as 0.5–2 μM decreased glycogen levels in insulin-stimulated primary murine hepatocytes by interfering with rate-limiting glycogenesis genes GS and GP and increasing glucose output (Zhang et al. 2017). Both arsenite and $MMA^{III}+$ down-regulated GS and up-regulated GP, in addition to inhibiting AKT phosphorylation, insulin's regulatory step for glycogen synthesis (Zhang et al. 2017). This finding parallels results of arsenic-treated adipocytes, with impaired AKT-dependent GLUT4 mobilization in trivalent arsenical-treated 3T3-L1 preadipocytes (Walton et al. 2004).

3T3-L1 preadipocytes, adipose-derived stromal vascular fraction cells (ADSVFCs), and human adipose tissue-derived stem cells (hADSCs), treated with low concentrations of $DMA^{III}+$ (≤2 μM) or $MMA^{III}+$ (≤1 μM), all experienced impaired adipogenesis mediated by UPR and ER stress (Hou et al. 2013). While arsenite and $MMA^{III}+$ interfered with adipogenesis via CHOP10 in the early stages of differentiation, $DMA^{III}+$ did not, suggesting its antiadipogenic effects are mediated via a different target (Hou et al. 2013). In addition, greater cytotoxicity was observed for both $MMA^{III}+$ and $DMA^{III}+$ in 3T3-L1 preadipocytes, SVCs, and hADSCs compared to arsenite (Hou et al. 2013). Future research should focus on the specific effects of trivalent arsenical metabolites on metabolic pathways to increase our understanding of the diabetogenic potential of arsenic metabolism and its intermediates.

Discussion

Our review of the literature on the laboratory research of arsenite exposure and its effects on glucose homeostasis suggests that several mechanisms may be involved, including insulin-stimulated glucose uptake, glucose-stimulated insulin secretion, hepatic glucose metabolism, and adipose and pancreatic β-cell dysfunction. Arsenite has wide physiological effects, affecting multiple metabolic organs involved in glucose homeostasis. Although the effects of arsenic exposure on the integrity and the physiology of various tissues are reported (Figure 3), the molecular mechanisms underlying these findings are mostly unknown. The *in vitro* studies and targets identified via omic databases of publicly available data have the potential to unravel these mechanisms. Different strains of rodents that respond to arsenic differently could also be used. The expert panel assembled by the NTP has therefore encouraged researchers to assess arsenic's metabolic effects in strains susceptible to these metabolic end points (Maull et al. 2012).

Current advances in omics technologies have been paralleled with the use of publicly available databases. Together, these tools have the ability to expand our understanding of chemically induced diseases. A recent study on the use of the CTD for the creation of adverse outcome pathways assessed arsenical exposures and dysregulation of glucose homeostasis as one of its primary case studies (Davis et al. 2018). This further emphasizes the relevance of elucidating potential mechanisms of action for a relevant topic in the fields of comparative toxicogenomics and environmental epidemiology (Davis et al. 2018). We were able to identify 16 genes commonly affected by sodium arsenite, insulin resistance, and T2D. A potential limitation of using specific key terms is the potential of missing relevant genes, exemplified by the hypermethylation of potassium voltage-gated channel subfamily Q member 1 (KCNQ1), a gene involved in insulin secretion that did not appear in our original search. Despite this limitation, MeSH identifiers continue to be widely used based on narrow research criteria.

Evidence from *in vitro* and *in vivo* studies suggest that arsenite interferes with signaling involved in glucose uptake and insulin secretion, down-regulating molecular targets such as AKT and glucose transporters (GLUT1, GLUT3, and GLUT4), and calcium signaling pathways involved in insulin exocytosis and secretion from pancreatic β cells, respectively (Figures 6 and 7). Arsenite has been shown to interfere with adipogenesis, which has implications for altered energy storage (Rosen and Spiegelman 2006). Hepatic manifestations are also present upon exposure, with the up-regulation of PCK1 and other rate-limiting enzymes of gluconeogenesis (Liu et al. 2014). Trivalent methylated arsenical metabolites MMA and DMA share similar effects to their parent compound, interfering with metabolic pathways involved in glucose homeostasis (Zhang et al. 2017; Hou et al. 2013; Douillet et al. 2013).

The 16 genes identified in our CTD analysis encode proteins that are involved in glucose homeostasis, oxidative stress, inflammation, lipid metabolism, energy balance, lipid metabolism, and adipogenesis, among other processes. Among the genes identified, insulin, insulin receptor, insulin receptor substrate 1 and 2 (IRS1 and IRS2, respectively), and Solute Carrier Family 2 Member 4 (SLC2A4) (also known as GLUT4) are components of the insulin signaling pathway that regulate glucose utilization in peripheral tissues (Rosen and Spiegelman 2006). Leptin and leptin receptor are components of leptin signaling, which increases satiety and controls energy balance. PPARγ encodes a nuclear receptor that positively regulates insulin sensitivity (Rosen and Spiegelman 2006). Thiazolidinediones, a class of antidiabetic drugs, act as agonists of PPARγ (Tontonoz and Spiegelman 2008). As discussed above, adiponectin (ADIPOQ) encodes a hormone secreted from white adipose tissue that improves insulin sensitivity (Rosen and Spiegelman 2006). An additional five genes (C3, TNF, NOS3, HMOX1, and SOD2) encode proteins involved in the inflammatory response. SOD2 (MnSOD) protein also clears mitochondrial ROS to reduce oxidative stress (Padmaja Divya et al. 2015). Interestingly, this analysis suggests that advanced glycosylated end products bind to their receptors, which can activate inflammatory pathways. Altogether, these genes provide strong evidence to support the association between arsenic dysregulation in various metabolic tissues.

There remains a need to critically determine which *in vitro* and *in vivo* study designs are most relevant to human exposures. The expression of As3MT in different cell lines may vary substantially, impacting the kinetics of arsenite metabolism and its effects in targets involved in glucose homeostasis. The assessment of sodium arsenite metabolism in four animal species, including rat, hamster, guinea pig, and mouse, found mice to be the most appropriate model to evaluate arsenic toxicity (Mitchell et al. 2000). While mice metabolize arsenic more quickly than humans, they have similar distribution parameters (Mitchell et al. 2000). Since arsenic metabolism kinetics differ between animal models and humans, calculations based solely on allometric scaling may not be valid and therefore are usually not reported (States et al. 2011). The limitation of using mouse models is commonly due to low biological sample availability (e.g., plasma, urine, tissue) due to the animal's small mass (Mitchell et al. 2000). Rats are considered a less appropriate animal model for arsenic metabolism as a proxy for human exposures than other mammalian models (ATSDR 2007; Lu et al. 2004; Mitchell et al. 2000). While circulating DMA^{III+} inorganic arsenic metabolite is accumulated in erythrocytes in rats, humans experience arsenic retention in epithelial tissues, such as the skin and lung (Lu et al. 2004).

Rodents either metabolize arsenic quicker or sequester it in blood cells and thus require concentrations of arsenic above those found in exposed populations to achieve similar internal doses (Maull et al. 2012). However, few studies report internal dose calculations, which require comprehensive water consumption estimates (States et al. 2011). The current literature also includes a broad duration of exposure periods, ranging from a few days to years (Maull et al. 2012). Routes of arsenic administration also vary and include oral exposure via drinking water, oral gavage, and intraperitoneal injection (Maull et al. 2012). The use of genetic biomarkers and histopathology of select tissues have instead been more widely employed to convey equivalence to arsenic toxicity in humans (States et al. 2011).

Conclusions

While epidemiology studies have linked arsenic exposure to the development of T2D in populations worldwide, the current mechanism by which arsenic contributes to dysregulation of glucose homeostasis remains elusive in humans despite well-established laboratory models. In the last two decades, efforts have focused on assessing arsenic's effects on metabolic target tissues, including the pancreas, adipose, liver, and skeletal muscle. Most *in vivo* studies have relied on rodents, administering higher arsenite concentrations at parts-per-million levels due to the species' accelerated arsenic metabolism compared to humans. Nonetheless, it is critical to model our experimental designs to internal doses that are relevant to human health and exposures. Human exposure assessment is also limited by the measurement of total arsenic concentration, which also includes organic arsenicals that are not considered hazardous to human health and irrelevant to toxicity associated with inorganic arsenic exposures.

Inconsistencies in the literature highlight the need for additional research characterizing the metabolic effects at chronic, low-dose exposures. High-exposure *in vivo* studies have shown that arsenic treatment alone can reduce GSIS (Liu et al. 2014; Kirkley

et al. 2017; Lee et al. 2014). High-exposure *in vivo* studies report arsenic treatment alone to affect glucose homeostasis by damaging the integrity of the pancreas, interfering with GSIS (Liu et al. 2014). However, lower-dose arsenite treatment alone has been found to exacerbate genetic and diet-induced insulin resistance and impaired glucose tolerance (Liu et al. 2014; Ditzel et al. 2016; Paul et al. 2011). *In vitro* studies of pancreatic β cells mostly confirm that high-dose arsenic exposure increases apoptosis, whereas low-dose arsenic inhibits GSIS (Pan et al. 2013; Lu et al. 2011; Díaz-Villaseñor et al. 2008). Many other *in vitro* results, however, require the corroboration of *in vivo* studies. For example, arsenic has been shown to affect ISGU in adipocytes and myotubes, increasing the breakdown of glycogen in hepatocytes and inhibiting insulin signaling in these cell types (Padmaja Divya et al. 2015). However, the effects of arsenic on peripheral glucose utilization and hepatic glucose production and insulin signaling *in vivo* have not been extensively explored. Another area of increasing interest is the interaction between arsenic and obesity, as an excess body mass index is a causal factor for T2D development. A recent study suggested a synergistic relationship with chronic arsenic exposure and obesity on T2D, with obese individuals being the most susceptible to T2D development (Castriota et al. 2018).

We used publicly available omics data and performed pathway identification using online tools to validate the relationship between arsenic and T2D, complementing experimental findings. This analysis resulted in the identification of key genes and pathways involved in arsenite-induced insulin. These data-driven approaches can assist researchers to harmonize, summarize, and structure existing mechanistic knowledge underlying arsenite-induced dysregulation of glucose homeostasis. These techniques can identify knowledge gaps and aid in the development of more focused study designs.

Insulin resistance is a chronic condition with epidemic proportions. The increasing prevalence of T2D both domestically and worldwide, in addition to arsenic's widespread exposure, motivates our efforts to determine arsenic's contribution to the etiology of this metabolic disorder (Zimmet et al. 2016). We hope this review will help to inform public health interventions due to the growing burden of T2D and ongoing arsenic exposure in vulnerable communities worldwide.

Acknowledgments

This work was supported by National Institutes of Health (NIH) grant P42ES004705 from the Superfund Research Program of the National Institute of Environmental Health Sciences [to the University of California, Berkeley (UC Berkeley)], NIH grants R01 ES014032 and R01DK113019 from the National Institute of Environmental Health Sciences and National Institute of Diabetes and Digestive and Kidney Diseases (to UC Berkeley), and the U.S. Department of Agriculture (USDA) National Institute of Food and Agriculture, Hatch Project 1002182 from the USDA National Institute of Food and Agriculture (to UC Davis).

References

Adebayo AO, Zandbergen F, Kozul-Horvath CD, Gruppuso PA, Hamilton JW. 2015. Chronic exposure to low-dose arsenic modulates lipogenic gene expression in mice: arsenic effect on lipid-regulating genes. J Biochem Mol Toxicol 29(1):1–9, PMID: 25155036, https://doi.org/10.1002/jbt.21600.

Agusa T, Fujihara J, Takeshita H, Iwata H. 2011. Individual variations in inorganic arsenic metabolism associated with AS3MT genetic polymorphisms. Int J Mol Sci 12(4):2351–2382, PMID: 21731446, https://doi.org/10.3390/ijms12042351.

Ambrosio F, Brown E, Stolz D, Ferrari R, Goodpaster B, Deasy B, et al. 2014. Arsenic induces sustained impairment of skeletal muscle and muscle progenitor cell ultrastructure and bioenergetics. Free Radic Biol Med 74:64–73, PMID: 24960579, https://doi.org/10.1016/j.freeradbiomed.2014.06.012.

ATSDR (Agency for Toxic Substances and Disease Registry). 2007. *Toxicological Profile for Arsenic*. Atlanta, GA: Agency for Toxic Substances and Disease Registry, Division of Toxicology and Environmental Medicine/Applied Toxicology Branch.

Bae J, Jang Y, Kim H, Mahato K, Schaecher C, Kim IM, et al. 2019. Arsenite exposure suppresses adipogenesis, mitochondrial biogenesis and thermogenesis via autophagy inhibition in brown adipose tissue. Sci Rep 9(1):14464, PMID: 31594991, https://doi.org/10.1038/s41598-019-50965-9.

Basu R, Basu A, Johnson CM, Schwenk WF, Rizza RA. 2004. Insulin dose-response curves for stimulation of splanchnic glucose uptake and suppression of endogenous glucose production differ in nondiabetic humans and are abnormal in people with type 2 diabetes. Diabetes 53(8):2042–2050, PMID: 15277384, https://doi.org/10.2337/diabetes.53.8.2042.

Beezhold K, Klei LR, Barchowsky A. 2017. Regulation of cyclin D1 by arsenic and microRNA inhibits adipogenesis. Toxicol Lett 265:147–155, PMID: 27932253, https://doi.org/10.1016/j.toxlet.2016.12.002.

Bindea G, Mlecnik B, Hackl H, Charoentong P, Tosolini M, Kirilovsky A, et al. 2009. ClueGO: a Cytoscape plug-in to decipher functionally grouped gene ontology and pathway annotation networks. Bioinformatics 25(8):1091–1093, PMID: 19237447, https://doi.org/10.1093/bioinformatics/btp101.

Castriota F, Acevedo J, Ferreccio C, Smith AH, Liaw J, Smith MT, et al. 2018. Obesity and increased susceptibility to arsenic-related type 2 diabetes in Northern Chile. Environ Res 167:248–254, PMID: 30059859, https://doi.org/10.1016/j.envres.2018.07.022.

Ceja-Galicia ZA, Daniel A, Salazar AM, Pánico P, Ostrosky-Wegman P, Díaz-Villaseñor A. 2017. Effects of arsenic on adipocyte metabolism: is arsenic an obesogen?. Mol Cell Endocrinol 452:25–32, PMID: 28495457, https://doi.org/10.1016/j.mce.2017.05.008.

Coelho M, Oliveira T, Fernandes R. 2013. Biochemistry of adipose tissue: an endocrine organ. Arch Med Sci 9(2):191–200, PMID: 23671428, https://doi.org/10.5114/aoms.2013.33181.

Cui Q, Fu J, Hu Y, Li Y, Yang B, Li L, et al. 2017. Deficiency of long isoforms of Nfe2l1 sensitizes MIN6 pancreatic β cells to arsenite-induced cytotoxicity. Toxicol Appl Pharmacol 329:67–74, PMID: 28549828, https://doi.org/10.1016/j.taap.2017.05.013.

Davis AP, Grondin CJ, Johnson RJ, Sciaky D, King BL, McMorran R, et al. 2017. The Comparative Toxicogenomics Database: update 2017. Nucleic Acids Res 45(D1):D972–D978, PMID: 27651457, https://doi.org/10.1093/nar/gkw838.

Davis AP, Wiegers TC, Wiegers J, Johnson RJ, Sciaky D, Grondin CJ, et al. 2018. Chemical-induced phenotypes at CTD help inform the pre-disease state and construct adverse outcome pathways. Toxicol Sci 165(1):145–156, PMID: 29846728, https://doi.org/10.1093/toxsci/kfy131.

DeFronzo RA. 2009. From the triumvirate to the ominous octet: a new paradigm for the treatment of type 2 diabetes mellitus. Diabetes 58(4):773–795, PMID: 19336687, https://doi.org/10.2337/db09-9028.

Díaz-Villaseñor A, Burns AL, Salazar AM, Sordo M, Hiriart M, Cebrián ME, et al. 2008. Arsenite reduces insulin secretion in rat pancreatic β-cells by decreasing the calcium-dependent calpain-10 proteolysis of SNAP-25. Toxicol Appl Pharmacol 231(3):291–299, PMID: 18597805, https://doi.org/10.1016/j.taap.2008.05.018.

Díaz-Villaseñor A, Sánchez-Soto MC, Cebrián ME, Ostrosky-Wegman P, Hiriart M. 2006. Sodium arsenite impairs insulin secretion and transcription in pancreatic β-cells. Toxicol Appl Pharmacol 214(1):30–34, PMID: 16413591, https://doi.org/10.1016/j.taap.2005.11.015.

Ditzel EJ, Nguyen T, Parker P, Camenisch TD. 2016. Effects of arsenite exposure during fetal development on energy metabolism and susceptibility to diet-induced fatty liver disease in male mice. Environ Health Perspect 124(2):201–209, PMID: 26151952, https://doi.org/10.1289/ehp.1409501.

Douillet C, Currier J, Saunders J, Bodnar WM, Matoušek T, Stýblo M. 2013. Methylated trivalent arsenicals are potent inhibitors of glucose stimulated insulin secretion by murine pancreatic islets. Toxicol Appl Pharmacol 267(1):11–15, PMID: 23261974, https://doi.org/10.1016/j.taap.2012.12.007.

Dover EN, Beck R, Huang MC, Douillet C, Wang Z, Klett EL, et al. 2018. Arsenite and methylarsonite inhibit mitochondrial metabolism and glucose-stimulated insulin secretion in INS-1 832/13 β cells. Arch Toxicol 92(2):693–704, PMID: 28956099, https://doi.org/10.1007/s00204-017-2074-y.

Druwe IL, Sollome JJ, Sanchez-Soria P, Hardwick RN, Camenisch TD, Vaillancourt RR. 2012. Arsenite activates NFκB through induction of C-reactive protein. Toxicol Appl Pharmacol 261(3):263–270, PMID: 22521605, https://doi.org/10.1016/j.taap.2012.04.005.

Farzan SF, Howe CG, Zens MS, Palys T, Channon JY, Li Z, et al. 2017. Urine arsenic and arsenic metabolites in U.S. adults and biomarkers of inflammation, oxidative stress, and endothelial dysfunction: a cross-sectional study. Environ Health Perspect 125(12):127002, PMID: 29373859, https://doi.org/10.1289/EHP2062.

Fu J, Woods CG, Yehuda-Shnaidman E, Zhang Q, Wong V, Collins S, et al. 2010. Low-level arsenic impairs glucose-stimulated insulin secretion in pancreatic beta cells: involvement of cellular adaptive response to oxidative stress. Environ Health Perspect 118(6):864–870, PMID: 20100676, https://doi.org/10.1289/ehp.0901608.

Garciafigueroa DY, Klei LR, Ambrosio F, Barchowsky A. 2013. Arsenic-stimulated lipolysis and adipose remodeling is mediated by G-protein-coupled receptors. Toxicol Sci 134(2):335–344, PMID: 23650128, https://doi.org/10.1093/toxsci/kft108.

Gentry PR, Covington TR, Mann S, Shipp AM, Yager JW, Clewell HJ 3rd. 2004. Physiologically based pharmacokinetic modeling of arsenic in the mouse. J Toxicol Environ Health A 67(1):43–71, PMID: 14668111, https://doi.org/10.1080/15287390490253660.

Grau-Perez M, Kuo CC, Gribble MO, Balakrishnan P, Jones Spratlen M, Vaidya D, et al. 2017. Association of low-moderate arsenic exposure and arsenic metabolism with incident diabetes and insulin resistance in the Strong Heart Family Study. Environ Health Perspect 125(12):127004, PMID: 29373862, https://doi.org/10.1289/EHP2566.

Hamann I, Petroll K, Hou X, Anwar-Mohamed A, El-Kadi AOS, Klotz LO. 2014. Acute and long-term effects of arsenite in HepG2 cells: modulation of insulin signaling. Biometals 27(2):317–332, PMID: 24535192, https://doi.org/10.1007/s10534-014-9714-y.

Hasnain SZ, Prins JB, McGuckin MA. 2016. Oxidative and endoplasmic reticulum stress in β-cell dysfunction in diabetes. J Mol Endocrinol 56(2):R33–R54, PMID: 26576641, https://doi.org/10.1530/JME-15-0232.

Hayakawa T, Kobayashi Y, Cui X, Hirano S. 2005. A new metabolic pathway of arsenite: arsenic-glutathione complexes are substrates for human arsenic methyltransferase Cyt19. Arch Toxicol 79(4):183–191, PMID: 15526190, https://doi.org/10.1007/s00204-004-0620-x.

Hectors TLM, Vanparys C, van der Ven K, Martens GA, Jorens PG, Van Gaal LF, et al. 2011. Environmental pollutants and type 2 diabetes: a review of mechanisms that can disrupt beta cell function. Diabetologia 54(6):1273–1290, PMID: 21442161, https://doi.org/10.1007/s00125-011-2109-5.

Hong GM, Bain LJ. 2012. Sodium arsenite represses the expression of myogenin in C2C12 mouse myoblast cells through histone modifications and altered expression of Ezh2, Glp, and Igf-1. Toxicol Appl Pharmacol 260(3):250–259, PMID: 22426358, https://doi.org/10.1016/j.taap.2012.03.002.

Hou Y, Xue P, Woods CG, Wang X, Fu J, Yarborough K, et al. 2013. Association between arsenic suppression of adipogenesis and induction of CHOP10 via the endoplasmic reticulum stress response. Environ Health Perspect 121(2):237–243, PMID: 23221991, https://doi.org/10.1289/ehp.1205731.

Hu Y, Jin X, Snow ET. 2002. Effect of arsenic on transcription factor AP-1 and NF-κB DNA binding activity and related gene expression. Toxicol Lett 133(1):33–45, PMID: 12076508, https://doi.org/10.1016/s0378-4274(02)00083-8.

Huang CF, Chen YW, Yang CY, Tsai KS, Yang RS, Liu SH. 2011. Arsenic and diabetes: current perspectives. Kaohsiung J Med Sci 27(9):402–410, PMID: 21914528, https://doi.org/10.1016/j.kjms.2011.05.008.

Hughes MF, Beck BD, Chen Y, Lewis AS, Thomas DJ. 2011. Arsenic exposure and toxicology: a historical perspective. Toxicol Sci 123(2):305–332, PMID: 21750349, https://doi.org/10.1093/toxsci/kfr184.

Hutton JC, O'Brien RM. 2009. Glucose-6-phosphatase catalytic subunit gene family. J Biol Chem 284(43):29241–29245, PMID: 19700406, https://doi.org/10.1074/jbc.R109.025544.

Keane KN, Cruzat VF, Carlessi R, de Bittencourt PIH Jr, Newsholme P. 2015. Molecular events linking oxidative stress and inflammation to insulin resistance and β-cell dysfunction. Oxid Med Cell Longev 2015:181643–181615, PMID: 26257839, https://doi.org/10.1155/2015/181643.

Kershaw EE, Flier JS. 2004. Adipose tissue as an endocrine organ. J Clin Endocrinol Metab 89(6):2548–2556, PMID: 15181022, https://doi.org/10.1210/jc.2004-0395.

Kirkley AG, Carmean CM, Ruiz D, Ye H, Regnier SM, Poudel A, et al. 2017. Arsenic exposure induces glucose intolerance and alters global energy metabolism. Am J Physiol Regul Integr Comp Physiol 314(2):R294–R303, PMID: 29118024, https://doi.org/10.1152/ajpregu.00522.2016.

Klei LR, Garciafigueroa DY, Barchowsky A. 2012. Arsenic activates endothelin-1 Gi protein–coupled receptor signaling to inhibit stem cell differentiation in adipogenesis. Toxicol Sci 131(2):512–520, PMID: 23152186, https://doi.org/10.1093/toxsci/kfs323.

Lee YS, Lee EK, Oh HH, Choi CS, Kim S, Jun HS. 2014. Sodium meta-arsenite ameliorates hyperglycemia in obese db/db mice by inhibition of hepatic gluconeogenesis. J Diabetes Res 2014:961732, PMID: 25610880, https://doi.org/10.1155/2014/961732.

Liu S, Guo X, Wu B, Yu H, Zhang X, Li M. 2014. Arsenic induces diabetic effects through beta-cell dysfunction and increased gluconeogenesis in mice. Sci Rep 4:6894, PMID: 25367288, https://doi.org/10.1038/srep06894.

Lotia S, Montojo J, Dong Y, Bader GD, Pico AR. 2013. Cytoscape app store. Bioinformatics 29(10):1350–1351, PMID: 23595664, https://doi.org/10.1093/bioinformatics/btt138.

Lu M, Wang H, Li X-F, Lu X, Cullen WR, Arnold LL, et al. 2004. Evidence of hemoglobin binding to arsenic as a basis for the accumulation of arsenic in rat blood. Chem Res Toxicol 17(12):1733–1742, PMID: 15606151, https://doi.org/10.1021/tx049756s.

Lu TH, Su CC, Chen YW, Yang CY, Wu CC, Hung DZ, et al. 2011. Arsenic induces pancreatic β-cell apoptosis via the oxidative stress-regulated mitochondria-dependent and endoplasmic reticulum stress-triggered signaling pathways. Toxicol Lett 201(1):15–26, PMID: 21145380, https://doi.org/10.1016/j.toxlet.2010.11.019.

Marshall C, Hitman GA, Partridge CJ, Clark A, Ma H, Shearer TR, et al. 2005. Evidence that an isoform of calpain-10 is a regulator of exocytosis in pancreatic beta-cells. Mol Endocrinol 19(1):213–224, PMID: 15471947, https://doi.org/10.1210/me.2004-0064.

Masuda Y, Vaziri ND, Li S, Le A, Hajighasemi-Ossareh M, Robles L, et al. 2015. The effect of Nrf2 pathway activation on human pancreatic islet cells. PLoS One 10(6):e0131012, PMID: 26110640, https://doi.org/10.1371/journal.pone.0131012.

Maull EA, Ahsan H, Edwards J, Longnecker MP, Navas-Acien A, Pi J, et al. 2012. Evaluation of the association between arsenic and diabetes: a National Toxicology Program workshop review. Environ Health Perspect 120(12):1658–1670, PMID: 22889723, https://doi.org/10.1289/ehp.1104579.

MDI Biological Laboratory. 2019. Comparative Toxicogenomics Database. http://ctdbase.org/ [accessed 15 August 2018].

Mitchell RD, Ayala-Fierro F, Carter DE. 2000. Systemic indicators of inorganic arsenic toxicity in four animal species. J Toxicol Environ Health A 59(2):119–134, PMID: 10653439, https://doi.org/10.1080/009841000157014.

Naujokas MF, Anderson B, Ahsan H, Aposhian HV, Graziano JH, Thompson C, et al. 2013. The broad scope of health effects from chronic arsenic exposure: update on a worldwide public health problem. Environ Health Perspect 121(3):295–302, PMID: 23458756, https://doi.org/10.1289/ehp.1205875.

Navas-Acien A, Silbergeld EK, Streeter RA, Clark JM, Burke TA, Guallar E. 2005. Arsenic exposure and type 2 diabetes: a systematic review of the experimental and epidemiologic evidence. Environ Health Perspect 114(5):641–648, PMID: 16675414, https://doi.org/10.1289/ehp.8551.

Noman ASM, Dilruba S, Mohanto NC, Rahman L, Khatun Z, Riad W, et al. 2015. Arsenic-induced histological alterations in various organs of mice. J Cytol Histol 6(3):323, PMID: 26740907, https://doi.org/10.4172/2157-7099.1000323.

OHAT (Office of Health Assessment and Translation). 2015. *OHAT Risk of Bias Rating Tool for Human and Animal Studies*. https://ntp.niehs.nih.gov/ntp/ohat/pubs/riskofbiastool_508.pdf.

Padmaja Divya S, Pratheeshkumar P, Son YO, Vinod Roy R, Andrew Hitron J, Kim D, et al. 2015. Arsenic induces insulin resistance in mouse adipocytes and myotubes via oxidative stress-regulated mitochondrial Sirt3-FOXO3a signaling pathway. Toxicol Sci 146(2):290–300, PMID: 25979314, https://doi.org/10.1093/toxsci/kfv089.

Pan X, Jiang L, Zhong L, Geng C, Jia L, Liu S, et al. 2016. Arsenic induces apoptosis by the lysosomal-mitochondrial pathway in INS-1 cells. Environ Toxicol 31(2):133–141, PMID: 25077447, https://doi.org/10.1002/tox.22027.

Pan WC, Seow WJ, Kile ML, Hoffman EB, Quamruzzaman Q, Rahman M, et al. 2013. Association of low to moderate levels of arsenic exposure with risk of type 2 diabetes in Bangladesh. Am J Epidemiol 178(10):1563–1570, PMID: 24049161, https://doi.org/10.1093/aje/kwt195.

Paul DS, Devesa V, Hernandez-Zavala A, Adair BM, Walton FS, Drobnâ Z, et al. 2008. Environmental arsenic as a disruptor of insulin signaling. Met Ions Biol Med 10:1–7, PMID: 20467584.

Paul DS, Hernández-Zavala A, Walton FS, Adair BM, Dědina J, Matoušek T, et al. 2007. Examination of the effects of arsenic on glucose homeostasis in cell culture and animal studies: development of a mouse model for arsenic-induced diabetes. Toxicol Appl Pharmacol 222(3):305–314, PMID: 17336358, https://doi.org/10.1016/j.taap.2007.01.010.

Paul DS, Walton FS, Saunders RJ, Stýblo M. 2011. Characterization of the impaired glucose homeostasis produced in C57BL/6 mice by chronic exposure to arsenic and high-fat diet. Environ Health Perspect 119(8):1104–1109, PMID: 21592922, https://doi.org/10.1289/ehp.1003324.

Peng Q, Harlow SD, Park SK. 2015. Urinary arsenic and insulin resistance in US adolescents. Int J Hyg Environ Health 218(4):407–413, PMID: 25845984, https://doi.org/10.1016/j.ijheh.2015.03.006.

Petersen MC, Vatner DF, Shulman GI. 2017. Regulation of hepatic glucose metabolism in health and disease. Nat Rev Endocrinol 13(10):572–587, PMID: 28731034, https://doi.org/10.1038/nrendo.2017.80.

Petrick JS, Ayala-Fierro F, Cullen WR, Carter DE, Vasken Aposhian H. 2000. Monomethylarsonous acid (MMA(III)) is more toxic than arsenite in Chang human hepatocytes. Toxicol Appl Pharmacol 163(2):203–207, PMID: 10698679, https://doi.org/10.1006/taap.1999.8872.

Pilkis SJ, Granner DK. 1992. Molecular physiology of the regulation of hepatic gluconeogenesis and glycolysis. Annu Rev Physiol 54:885–909, PMID: 1562196, https://doi.org/10.1146/annurev.ph.54.030192.004321.

Renu K, Madhyastha H, Madhyastha R, Maruyama M, Arunachlam S, Abilash VG. 2018. Role of arsenic exposure in adipose tissue dysfunction and its possible implication in diabetes pathophysiology. Toxicol Lett 284:86–95, PMID: 29198881, https://doi.org/10.1016/j.toxlet.2017.11.032.

Rodríguez VM, Limón-Pacheco JH, Del Razo LM, Giordano M. 2016. Effects of inorganic arsenic exposure on glucose transporters and insulin receptor in the hippocampus of C57BL/6 male mice. Neurotoxicol Teratol 54:68–77, PMID: 26876454, https://doi.org/10.1016/j.ntt.2016.02.001.

Rosen ED, MacDougald OA. 2006. Adipocyte differentiation from the inside out. Nat Rev Mol Cell Biol 7(12):885–896, PMID: 17139329, https://doi.org/10.1038/nrm2066.
Rosen ED, Spiegelman BM. 2006. Adipocytes as regulators of energy balance and glucose homeostasis. Nature 444(7121):847–853, PMID: 17167472, https://doi.org/10.1038/nature05483.
Saltiel AR, Kahn CR. 2001. Insulin signalling and the regulation of glucose and lipid metabolism. Nature 414(6865):799–806, PMID: 11742412, https://doi.org/10.1038/414799a.
Shi X, Wei X, Koo I, Schmidt RH, Yin X, Kim SH, et al. 2014. Metabolomic analysis of the effects of chronic arsenic exposure in a mouse model of diet-induced fatty liver disease. J Proteome Res 13(2):547–554, PMID: 24328084, https://doi.org/10.1021/pr400719u.
Slenter DN, Kutmon M, Hanspers K, Riutta A, Windsor J, Nunes N, et al. 2018. WikiPathways: a multifaceted pathway database bridging metabolomics to other omics research. Nucleic Acids Res 46(D1):D661–D667, PMID: 29136241, https://doi.org/10.1093/nar/gkx1064.
Soga M, Matsuzawa A, Ichijo H. 2012. Oxidative stress-induced diseases via the ASK1 signaling pathway. Int J Cell Biol 2012:439587, PMID: 22654913, https://doi.org/10.1155/2012/439587.
Song X, Li Y, Liu J, Ji X, Zhao L, Wei Y. 2017. Changes in serum adiponectin in mice chronically exposed to inorganic arsenic in drinking water. Biol Trace Elem Res 179(1):140–147, PMID: 28190184, https://doi.org/10.1007/s12011-017-0950-1.
States JC, Barchowsky A, Cartwright IL, Reichard JF, Futscher BW, Lantz RC. 2011. Arsenic toxicology: translating between experimental models and human pathology. Environ Health Perspect 119(10):1356–1363, PMID: 21684831, https://doi.org/10.1289/ehp.1103441.
Styblo M, Del Razo LM, Vega L, Germolec DR, LeCluyse EL, Hamilton GA, et al. 2000. Comparative toxicity of trivalent and pentavalent inorganic and methylated arsenicals in rat and human cells. Arch Toxicol 74(6):289–299, PMID: 11005674, https://doi.org/10.1007/s002040000134.
Sundaresan NR, Gupta M, Kim G, Rajamohan SB, Isbatan A, Gupta MP. 2009. Sirt3 blocks the cardiac hypertrophic response by augmenting Foxo3a-dependent antioxidant defense mechanisms in mice. J Clin Invest 119(9):2758–2771, PMID: 19652361, https://doi.org/10.1172/JCI39162.
Sztalryd C, Brasaemle DL. 2017. The perilipin family of lipid droplet proteins: gatekeepers of intracellular lipolysis. Biochim Biophys Acta Mol Cell Biol Lipids 1862(10 Pt B):1221–1232, PMID: 28754637, https://doi.org/10.1016/j.bbalip.2017.07.009.
Tan M, Schmidt RH, Beier JI, Watson WH, Zhong H, States CJ, et al. 2011. Chronic subhepatoxic exposure to arsenic enhances hepatic injury caused by high fat diet in mice. Toxicol Appl Pharmacol 257(3):356–364, PMID: 21983427, https://doi.org/10.1016/j.taap.2011.09.019.
Thayer KA, Heindel JJ, Bucher JR, Gallo MA. 2012. Role of environmental chemicals in diabetes and obesity: a National Toxicology Program workshop review. Environ Health Perspect 120(6):779–789, PMID: 22296744, https://doi.org/10.1289/ehp.1104597.
Tontonoz P, Spiegelman BM. 2008. Fat and beyond: the diverse biology of PPARgamma. Annu Rev Biochem 77:289–312, PMID: 18518822, https://doi.org/10.1146/annurev.biochem.77.061307.091829.
Trouba KJ, Wauson EM, Vorce RL. 2000. Sodium arsenite inhibits terminal differentiation of murine C3H 10T1/2 preadipocytes. Toxicol Appl Pharmacol 168(1):25–35, PMID: 11000097, https://doi.org/10.1006/taap.2000.9012.
Walton FS, Harmon AW, Paul DS, Drobná Z, Patel YM, Styblo M. 2004. Inhibition of insulin-dependent glucose uptake by trivalent arsenicals: possible mechanism of arsenic-induced diabetes. Toxicol Appl Pharmacol 198(3):424–433, PMID: 15276423, https://doi.org/10.1016/j.taap.2003.10.026.
Wauson EM, Langan AS, Vorce RL. 2002. Sodium arsenite inhibits and reverses expression of adipogenic and fat cell-specific genes during in vitro adipogenesis. Toxicol Sci 65(2):211–219, PMID: 11812925, https://doi.org/10.1093/toxsci/65.2.211.
WikiPathways. 2018. WikiPathways Repository. Updated 2 February 2018. https://www.wikipathways.org/index.php/WikiPathways [accessed 14 February 2018].
Wu J, Liu J, Waalkes MP, Cheng ML, Li L, Li CX, et al. 2008. High dietary fat exacerbates arsenic-induced liver fibrosis in mice. Exp Biol Med (Maywood) 233(3):377–384, PMID: 18296743, https://doi.org/10.3181/0710-RM-269.
Wu W, Yao X, Jiang L, Zhang Q, Bai J, Qiu T, et al. 2018. Pancreatic islet-autonomous effect of arsenic on insulin secretion through endoplasmic reticulum stress-autophagy pathway. Food Chem Toxicol 111:19–26, PMID: 29111283, https://doi.org/10.1016/j.fct.2017.10.043.
Xu J, Kulkarni SR, Donepudi AC, More VR, Slitt AL. 2012. Enhanced Nrf2 activity worsens insulin resistance, impairs lipid accumulation in adipose tissue, and increases hepatic steatosis in leptin-deficient mice. Diabetes 61(12):3208–3218, PMID: 22936178, https://doi.org/10.2337/db11-1716.
Xue P, Hou Y, Zhang Q, Woods CG, Yarborough K, Liu H, et al. 2011. Prolonged inorganic arsenite exposure suppresses insulin-stimulated AKT S473 phosphorylation and glucose uptake in 3T3-L1 adipocytes: involvement of the adaptive antioxidant response. Biochem Biophys Res Commun 407(2):360–365, PMID: 21396911, https://doi.org/10.1016/j.bbrc.2011.03.024.
Yadav S, Anbalagan M, Shi Y, Wang F, Wang H. 2013. Arsenic inhibits the adipogenic differentiation of mesenchymal stem cells by down-regulating peroxisome proliferator-activated receptor gamma and CCAAT enhancer-binding proteins. Toxicol In Vitro 27(1):211–219, PMID: 23108036, https://doi.org/10.1016/j.tiv.2012.10.012.
Yang B, Fu J, Zheng H, Xue P, Yarborough K, Woods CG, et al. 2012. Deficiency in the nuclear factor E2-related factor 2 renders pancreatic β-cells vulnerable to arsenic-induced cell damage. Toxicol Appl Pharmacol 264(3):315–323, PMID: 23000044, https://doi.org/10.1016/j.taap.2012.09.012.
Yao XF, Zheng BL, Bai J, Jiang LP, Zheng Y, Qi BX, et al. 2015. Low-level sodium arsenite induces apoptosis through inhibiting TrxR activity in pancreatic β-cells. Environ Toxicol Pharmacol 40(2):486–491, PMID: 26291581, https://doi.org/10.1016/j.etap.2015.08.003.
Ye R, Scherer PE. 2013. Adiponectin, driver or passenger on the road to insulin sensitivity? Mol Metab 2(3):133–141, PMID: 24049728, https://doi.org/10.1016/j.molmet.2013.04.001.
Zhang C, Fennel EMJ, Douillet C, Stýblo M. 2017. Exposures to arsenite and methylarsonite produce insulin resistance and impair insulin-dependent glycogen metabolism in hepatocytes. Arch Toxicol 91(12):3811–3821, PMID: 28952001, https://doi.org/10.1007/s00204-017-2076-9.
Zimmet PK, Alberti G, Magliano DJ, Bennett PH. 2016. Diabetes mellitus statistics on prevalence and mortality: facts and fallacies. Nat Rev Endocrinol 12(10):616–622, PMID: 27388988, https://doi.org/10.1038/nrendo.2016.105.
Zuo Z, Liu Z, Gao T, Yin Y, Wang Z, Hou Y, et al. 2019. Prolonged inorganic arsenic exposure via drinking water impairs brown adipose tissue function in mice. Sci Total Environ 668:310–317, PMID: 30852208, https://doi.org/10.1016/j.scitotenv.2019.03.008.